

# TOWARDS SPECTRAL CONVERGENCE OF LOCALLY LINEAR EMBEDDING ON MANIFOLDS WITH BOUNDARY

ANDREW LYONS

**ABSTRACT.** We study the eigenvalues and eigenfunctions of a differential operator that governs the asymptotic behavior of the unsupervised learning algorithm known as Locally Linear Embedding when a large data set is sampled from an interval or disc. In particular, the differential operator is of second order, mixed-type, and degenerates near the boundary. We show that a natural regularity condition on the eigenfunctions imposes a consistent boundary condition and use the Frobenius method to estimate pointwise behavior. We then determine the limiting sequence of eigenvalues analytically and compare them to numerical predictions. Finally, we propose a variational framework for determining eigenvalues on other compact manifolds.

## 1. INTRODUCTION

We study the eigenvalues and eigenfunctions of a mixed-type differential operator that informs the behavior of the dimensional limit of the *Locally Linear Embedding* (LLE) matrix, as defined in [15, Sec.2]. Locally Linear Embedding is a nonlinear algorithm used in data science to reduce the dimension of a data set and has been widely used in a variety of scientific fields. Introduced by Roweis and Saul in 2000 [10], the objective is to determine a map from a subset of  $\mathbb{R}^{d_1}$  to  $\mathbb{R}^{d_2}$  where  $d_1 > d_2$  and the local geometry is preserved, as made precise in Section 2. The underlying idea is that by parametrizing a data set locally, one can recover another data set embedded in a lower dimensional space but with a similar local structure.

The Locally Linear Embedding algorithm has a wide range of applications, from medical classification [7, 11] to audiovisual processing [2, 16]. Related algorithms, such as diffusion maps, have been used to numerically estimate solutions to differential equations on compact manifolds with boundary [1, 13], and LLE has the potential to do the same. This work furthers an effort to understand the differential operator approximated by the LLE matrix  $W$  when a data set is sampled from a manifold with boundary and the number of data points is large [14, 15]. The differential operator of interest is piecewise defined over a smooth, compact Riemannian manifold with boundary and degenerates on a submanifold of codimension 1. The domain of the operator is not known a priori; however, we show how a regularity condition on the eigenfunctions enforces a boundary condition on the degenerate submanifold and present asymptotic properties of the eigenfunctions and eigenvalues.

Let  $(M, g)$  be a  $d$ -dimensional, smooth, compact Riemannian manifold with smooth boundary, isometrically embedded in  $\mathbb{R}^{d_1}$ . To avoid error from sample variance, we take our high-dimensional data set  $\{x_j\}_{j=1}^n$  along a uniform grid in  $M$ . Let  $\epsilon$  be the algorithmic parameter that determines the neighborhood size about each  $x_j$ , as introduced in Section 2. Smaller values of  $\epsilon$  generally improve the local parametrization of each  $x_j$  in LLE, but only if the number of data points  $n$  is sufficiently large. To ensure that this happens, we hereafter take  $\epsilon = \epsilon(n)$  to be supercritical, meaning

$$\lim_{n \rightarrow \infty} \epsilon(n) = 0 \quad \text{and} \quad \lim_{n \rightarrow \infty} n\epsilon^{d_1}(n) = \infty. \quad (1.1)$$

In [15], Wu and Wu found that, upon the regularization discussed in Section 2, the LLE matrix  $W \in \mathbb{R}^{n \times n}$  behaves like a second order, mixed-type differential operator as  $n \rightarrow \infty$ . More precisely, they proved that there exists a differential operator  $D_\epsilon$  such that for  $k \in \{1, \dots, n\}$ ,

$$\sum_{j=1}^n (I - W)_{kj} f(x_j) = \epsilon^2 D_\epsilon f(x_k) + O(\epsilon^3) \quad (1.2)$$

with probability greater than  $1 - n^{-2}$ . Note that we have deviated slightly from the presentation in [15, Thm.16] via a global sign change and omission of the variance error. The constant in the error term of (1.2) depends on the  $C^2$  norm of  $f$  and properties of the manifold  $M$ . For this reason, we are interested in understanding eigenpairs  $(\lambda, u) \in \mathbb{C} \times C^2(M)$  satisfying

$$D_\epsilon u = \lambda u \quad \text{on } M \quad (1.3)$$

for small  $\epsilon$ . However, it is not immediately clear whether this objective is well-defined. One curious aspect of (1.2) is the lack of apparent boundary conditions, which play no role in the finite-dimensional case. Motivated by [4, 6], we demonstrate how boundary conditions are naturally encoded in the function space  $C^2(M)$  and that the eigenvalues can be defined via a min-max principle.

An additional challenge is posed by the fact that  $D_\epsilon$  is mixed-type, changing from elliptic to hyperbolic in the boundary layer

$$M_\epsilon := \{x \in M : \text{dist}_g(x, \partial M) < \epsilon\} \quad (1.4)$$

as depicted in Figure 1. This is remedied by studying the solution locally and patching local solutions to form a global one. For a given manifold  $M$ , we set

$$\begin{aligned} M_+ &= \{x \in M : D_\epsilon \text{ is elliptic at } x\} \\ M_- &= \{x \in M : D_\epsilon \text{ is hyperbolic at } x\} \end{aligned} \quad (1.5)$$

with  $\Gamma$  denoting the boundary between the two regions, where  $D_\epsilon$  degenerates. In particular,  $\Gamma = \partial M_+$  is diffeomorphic to the boundary  $\partial M$ , and the hyperbolic region  $M_-$  is a subset of  $M_\epsilon$ .

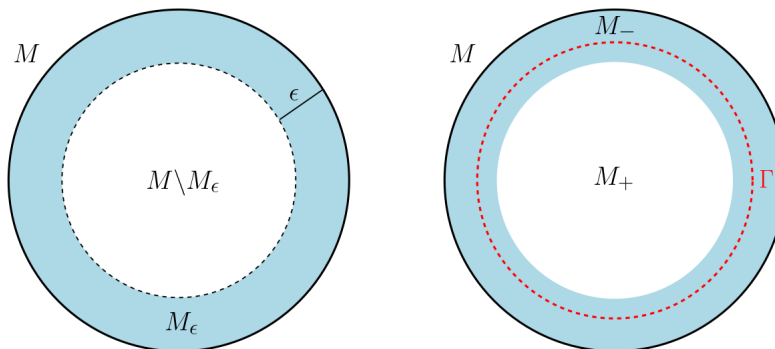


FIGURE 1. When  $M$  is the disc, the left figure depicts the boundary layer  $M_\epsilon$ , and the right figure depicts the elliptic and hyperbolic regions  $M_+, M_-$  separated by  $\Gamma$ .

A construction for  $D_\epsilon$  is presented in [15, Def. 12]. However, because (1.2) is pointwise, this construction relies on oriented normal coordinates at each point. For this reason, we analyze the differential operator on separable domains with a smooth boundary, where  $D_\epsilon$  can be defined globally. On the interval  $[0, 1]$ , (1.3) takes the Sturm-Liouville form

$$-(p_1(x)u'(x))' = \lambda w_1(x)u(x) \quad \text{for } x \in (0, 1), \quad (1.6)$$

where exact formulas for  $p_1, w_1$  are presented in Section 3. The principal coefficient  $p_1$  is continuous and sign-changing and hence defines the elliptic and hyperbolic regions in (1.5). Meanwhile, the weight  $w_1$  is continuous and positive over the interval. On the disc  $\overline{B_1(0)}$  with polar coordinates, (1.3) takes the form

$$-\frac{\partial}{\partial r} \left( p_2(1-r) \frac{\partial u}{\partial r}(r, \theta) \right) + q_2(1-r) \frac{\partial^2 u}{\partial \theta^2}(r, \theta) = \lambda w_2(1-r)u(r, \theta), \quad (1.7)$$

where exact formulas for  $p_2, q_2, w_2$  are presented in Section 4. As on the interval, the principal coefficient  $p_2$  is continuous and sign-changing and defines (1.5), while the weight  $w_2$  is continuous and positive over the disc. In particular,  $D_\epsilon$  degenerates where the principal coefficient vanishes.

For a general manifold,  $D_\epsilon$  simplifies to the Laplacian outside the boundary layer, reducing (1.3) to

$$-\frac{1}{2(d+2)} \Delta u = \lambda u \quad \text{on } M \setminus M_\epsilon$$

where  $d$  is the dimension of  $M$ . This is consistent with the LLE convergence result of [14], when  $M$  is a compact manifold without boundary. Because  $M_\epsilon$  vanishes as  $\epsilon \rightarrow 0$ , eigenfunctions of  $D_\epsilon$  behave asymptotically like eigenfunctions of the Laplacian. Using the explicit construction of  $D_\epsilon$  on the interval and disc, we determine a consistent boundary condition for the eigenfunctions of (1.3).

Equations (1.6) and (1.7) introduce the relevant notion of a quasi-derivative, as presented in [17]. Absent any regularity requirement, there may be solutions to (1.7) for which the quasi-derivative  $p_2(1-r) \frac{\partial u}{\partial r}(r, \theta)$  is differentiable but the derivative  $\frac{\partial u}{\partial r}(r, \theta)$  is not. By construction, the partial derivative  $\frac{\partial}{\partial r}$  serves as the normal derivative on  $\Gamma$ , so we interpret quasi-Neumann boundary conditions on  $M_+$  as being satisfied when

$$p_2(1-r) \frac{\partial u}{\partial r}(r, \theta) = 0 \quad \text{on } \Gamma.$$

Using (1.6) and (1.7), we present eigenvalue and eigenfunction properties that arise in (1.3) under the condition  $u \in C^2(M)$ . We then present a natural extension of this framework to other compact manifolds with boundary.

**1.1. Eigenfunction properties on the interval and disc.** In this section, we present results regarding the limiting eigenvalue sequence of  $D_\epsilon$  and discuss the natural boundary condition that corresponding eigenfunctions satisfy. We then present a variational interpretation of the eigenvalues that is consistent on both the interval and disc. The first result holds when  $D_\epsilon$  is defined on the unit interval and is proved in Section 3.2.

**Theorem 1.1.** *Let  $M$  be the unit interval  $[0, 1]$  and  $M_+ = \{x : p_1(x) > 0\}$  with  $p_1, w_1$  given in (1.6). There exists a constant  $\epsilon_0 > 0$  such that for all  $0 < \epsilon \leq \epsilon_0$ , the set of  $C^2(M)$  solutions to (1.3) coincides with eigenfunctions of  $D_\epsilon$  satisfying that for every  $y \in \partial M_+$ ,*

$$\lim_{x \rightarrow y} p_1(x)u'(x) = 0. \quad (1.8)$$

If (1.8) holds,

- (i)  $D_\epsilon$  is self-adjoint on  $L^2(M_+, w_1)$ .
- (ii) The spectrum is discrete with  $\sigma(D_\epsilon) \subset [0, \infty)$ .
- (iii) Constant functions form the kernel of  $D_\epsilon$ .

This result states that the regularity requirement forces a Neumann-type boundary condition on a subset of  $[0, 1]$  that converges to the whole interval as  $\epsilon$  vanishes. Further, the eigenvalue properties match those expected of the matrix  $I - W$  when the sampled data set in LLE is sufficiently large, as discussed in Section 2. For a precise estimate on the eigenvalues of  $D_\epsilon$  on the interval, see Corollary 3.5, and for a numerical

demonstration of spectral convergence on the interval, see Section 5. The second result holds when  $D_\epsilon$  is defined on the unit disc and is proved in Section 4.2.

**Theorem 1.2.** *Let  $M$  be the unit disc  $\overline{B_1(0)}$  and  $M_+ = \{(r, \theta) : p_2(1-r) > 0\}$  with  $p_2, w_2$  given in (1.7). There exists a constant  $\epsilon_0 > 0$  such that for all  $0 < \epsilon \leq \epsilon_0$ , the set of  $C^2(M)$  solutions to (1.3) coincides with eigenfunctions of  $D_\epsilon$  satisfying that for every  $y \in \partial M_+$ ,*

$$\lim_{(r, \theta) \rightarrow y} p_2(1-r) \frac{\partial u}{\partial r}(r, \theta) = 0. \quad (1.9)$$

If (1.9) holds,

- (i)  $D_\epsilon$  is self-adjoint on  $L^2(M_+, w_2)$ .
- (ii) The spectrum is discrete with  $\sigma(D_\epsilon) \subset [0, \infty)$ .
- (iii) Constant functions form the kernel of  $D_\epsilon$ .

Similar to Theorem 1.1, this result states that the same regularity requirement forces a Neumann-type boundary condition on a subset of  $\overline{B_1(0)}$  that converges to the whole disc as  $\epsilon$  vanishes. The eigenvalues mirror the limiting properties of  $I - W$  for large data sets. For a numerical demonstration of spectral convergence on the disc, see Section 5. The following statement presents the variational framework for eigenvalues of  $D_\epsilon$  on the interval (1.6) and is proved in Section 3.

**Theorem 1.3.** *Let  $M = [0, 1]$  and set*

$$V = \left\{ v \in L^2(M_+, w_1) : \int_{M_+} p_1(x) |v'(x)|^2 dx < \infty \right\}.$$

If the eigenfunctions of  $D_\epsilon$  on  $M$  satisfy (1.8), then the eigenvalues  $\{\lambda_j\}_j$  satisfy

$$\lambda_j = \max_{\substack{V_j \subseteq L^2(M_+, w_1), \\ |V_j| = j-1}} \left\{ \min_{v \in V \cap V_j^\perp \setminus \{0\}} \frac{\int_{M_+} p_1(x) |v'(x)|^2 dx}{\int_{M_+} w_1(x) |v(x)|^2 dx} \right\}$$

for all  $j \geq 1$ .

This result states that the eigenvalues of  $D_\epsilon$  can be determined via a min-max principle, in which an energy functional is varied over an appropriate function space. This method necessarily imposes quasi-Neumann boundary conditions on the minimizers and parallels the analogous finite-dimensional method for the matrix  $I - W$ . The next result holds when  $D_\epsilon$  is defined on the unit disc and is proved in Section 4.

**Theorem 1.4.** *Let  $M = \overline{B_1(0)}$  and set*

$$V = \left\{ v \in L^2(M_+, w_2) : \int_{M_+} p_2(1-r) \left| \frac{\partial v}{\partial r}(r, \theta) \right|^2 dr d\theta + \int_{M_+} q_2(1-r) \frac{\partial^2 v}{\partial \theta^2}(r, \theta) \overline{v(r, \theta)} dr d\theta < \infty \right\}.$$

If eigenfunctions of  $D_\epsilon$  on  $M$  satisfy (1.9), then the eigenvalues  $\{\lambda_j\}_j$  satisfy

$$\lambda_j = \max_{\substack{V_j \subseteq L^2(M_+, w_2), \\ |V_j| = j-1}} \left\{ \min_{v \in V \cap V_j^\perp \setminus \{0\}} \frac{\int_{M_+} p_2(1-r) \left| \frac{\partial v}{\partial r}(r, \theta) \right|^2 dr d\theta + \int_{M_+} q_2(1-r) \frac{\partial^2 v}{\partial \theta^2}(r, \theta) \overline{v(r, \theta)} dr d\theta}{\int_{M_+} w_2(1-r) |v(r, \theta)|^2 dr d\theta} \right\}$$

for all  $j \geq 1$ .

Analogous to Theorem 1.3, this statement provides the variational framework for interpreting eigenvalues on the disc. Motivated by Theorems 1.3 and 1.4, we consider the following weak construction for  $D_\epsilon$  when  $M$  is a general compact,  $d$ -dimensional Riemannian manifold with smooth boundary.

**Definition 1.5.** *We say  $D_\epsilon$  is admissible on  $M$  if there exist nonnegative functions  $p, w$  on  $M_+$  and a symmetric, nonnegative operator  $A_\epsilon$  on  $L^2(M_+ \cap M_\epsilon, w)$  such that*

$$\begin{aligned} \langle D_\epsilon u, v \rangle_{L^2(M_+, w)} &= \frac{1}{2(d+2)} \int_{M \setminus M_\epsilon} \nabla u(x) \overline{\nabla v(x)} dv_g \\ &\quad + \int_{M_+ \cap M_\epsilon} p(x_d) \frac{\partial u}{\partial x_d}(x) \overline{\frac{\partial v}{\partial x_d}(x)} dx \\ &\quad + \int_{M_+ \cap M_\epsilon} w(x_d) A_\epsilon u(x) \overline{v(x)} dx \end{aligned} \quad (1.10)$$

where  $\{x_1, \dots, x_d\}$  are Fermi coordinates [5, Ch. 2] such that  $x_d = 0$  along the boundary  $\partial M$  and  $x_d > 0$  in the interior of  $M$ . In addition,

$$\frac{1}{2(d+2)} \int_{\partial M_\epsilon} \frac{\partial u}{\partial \nu}(x) \overline{v(x)} d\sigma + p(\epsilon) \int_{\partial M_\epsilon} \frac{\partial u}{\partial x_d}(x', \epsilon) \overline{v(x', \epsilon)} dx' = 0 \quad (1.11)$$

where  $x = (x', x_d)$  in  $M_\epsilon$ ,  $\nu$  is the outward-pointing normal on  $\partial M_\epsilon$  and  $d\sigma$  is the measure on the boundary.

$D_\epsilon$  is necessarily admissible on both the interval and disc. The function  $p$  is meant to capture the degenerate behavior of  $D_\epsilon$  in the boundary layer, remaining positive on  $M_+$  and negative on  $M_-$ . As in Conjecture 1 below, we expect that the spectrum of  $D_\epsilon$  is completely described by the behavior of the differential operator on the elliptic region. Equation (1.11) is meant to stitch together the piecewise construction for  $D_\epsilon$ , which behaves like the Laplacian on  $M \setminus M_\epsilon$  but relies on Fermi coordinates in  $M_\epsilon$ .

Under Definition 1.5, a variational interpretation of the eigenvalues enforces a quasi-Neumann boundary condition on the eigenfunctions of  $D_\epsilon$  when defined over a general compact manifold. This is presented more precisely in the following statement, which is proved in Section 6.

**Theorem 1.6.** *Let  $M$  be a smooth, compact Riemannian manifold with smooth boundary and set*

$$V = \{v \in L^2(M_+, w) : \langle D_\epsilon v, v \rangle_{L^2(M_+, w)} < \infty\}.$$

*Let  $D_\epsilon$  be admissible on  $M$ . If the eigenvalues  $\{\lambda_j\}_j$  of  $D_\epsilon$  satisfy*

$$\lambda_j = \max_{\substack{V_j \subseteq L^2(M_+, w) \\ |V_j|=j-1}} \left\{ \min_{v \in V \cap V_j^\perp \setminus \{0\}} \frac{\langle D_\epsilon v, v \rangle_{L^2(M_+, w)}}{\langle v, v \rangle_{L^2(M_+, w)}} \right\},$$

*for all  $j \geq 1$ , then the corresponding eigenfunctions satisfy that for every  $y \in \partial M_+$ ,*

$$\lim_{x \rightarrow y} p(x_d) \frac{\partial u}{\partial x_d}(x) = 0. \quad (1.12)$$

By construction,  $-\frac{\partial}{\partial x_d}$  denotes the outward normal derivative along  $\partial M_+$ , and  $p$  is the principal coefficient that determines where  $D_\epsilon$  is elliptic. Thus,  $p$  vanishes along  $\Gamma$ , meaning that the quasi-Neumann boundary condition can be naturally interpreted as a statement regarding regularity. Namely, the conclusion of Theorem 1.6 states that the normal derivative of  $u$  does not blow up faster than  $p$  vanishes.

In [1], Coifman and Lafon provided the leading order asymptotics for the Graph Laplacian  $L \in \mathbb{R}^{n \times n}$  on manifolds with smooth boundary. In contrast to Wu and Wu's result for the LLE matrix [15, Thm. 16], they found that  $L$  behaved like a first order differential operator near the boundary, suggesting a Neumann boundary condition. This was later justified in [13, Thm. 6.2] when Vaughn, Berry, and Antil proved that

the Graph Laplacian converges weakly to the Dirichlet form. Namely,  $\sum_{k=1}^n \sum_{j=1}^n f(x_k) L_{kj} f(x_j)$  behaves like a multiple of  $\int_M |\nabla f(x)|^2 dv_g$  for large  $n$ . We expect that, when sampled on a generic smooth, compact manifold with boundary, the matrix  $I - W$  converges weakly to the form in (1.10).

**Conjecture 1.** *Let  $M$  be a Riemannian manifold with smooth boundary and suppose  $\{x_j\}_{j=1}^n$  is sampled along a uniform grid in  $M$ . If  $\epsilon = \epsilon(n)$  is supercritical, then  $D_\epsilon$  is admissible on  $M$  and the LLE matrix  $W$  satisfies*

$$\sum_{k=1}^n \sum_{j=1}^n f(x_k) (I - W)_{kj} f(x_j) = \epsilon^2 \frac{\langle D_\epsilon f, f \rangle_{L^2(M_+, w)}}{\|f\|_{L^2(M_+, w)}^2} + o(\epsilon^2).$$

In combination, Theorem 1.6 and Conjecture 1 provide a justification for the quasi-Neumann boundary condition (1.12) arising on general manifolds.

**1.2. Outline.** The structure of the paper is as follows. In Section 2, we detail the Locally Linear Embedding algorithm and the construction of the LLE matrix  $W$ . We highlight key properties that support the results of Theorem 1.1 and 1.2. In Section 3, we detail the operator  $D_\epsilon$  on the interval and use its form to determine the regularity of local solutions in the boundary layer. Using the Frobenius method, we isolate a unique eigenfunction and prove Theorem 1.1. We then present a variational framework for determining the spectrum and provide eigenvalue estimates. In Section 4, we present  $D_\epsilon$  on the unit disc and use a similar argument to prove Theorem 1.2. In particular, the boundary condition enforced by taking eigenfunctions in  $C^2(M)$  is consistent on both domains.

In Section 5, we corroborate Theorems 1.1 and 1.2 numerically, demonstrating eigenvalue convergence on both the interval and disc. More precisely, by constructing a piecewise approximation for the eigenfunctions of (1.3), we use the matching conditions presented in Propositions 3.4 and 4.4 to estimate the eigenvalues. In Section 6, we prove Theorem 1.6 under Definition 1.5. Finally, in Appendix A, we discuss how the  $C^2(M)$  regularity requirement might naturally arise from the higher order terms in (1.2) when  $M$  is the interval. We present an explicit differential operator that converges asymptotically to  $D_\epsilon$  but enforces high regularity for small  $\epsilon$ . Motivated by this example, we conclude with a conjecture regarding the higher order terms in (1.2) when  $M$  is a general compact manifold with boundary.

**1.3. Acknowledgments.** The author is grateful to Yaiza Canzani, Jeremy Marzuola, and Hau-Tieng Wu for helpful conversations regarding the featured problem. The author received support from NSF grants DMS-2045494 and DMS-1900519 as well as from NSF RTG DMS-2135998.

## 2. CONSTRUCTION AND PROPERTIES OF THE LLE MATRIX.

In this section, we briefly describe how the Locally Linear Embedding matrix is constructed and its purpose in the LLE algorithm. For a more detailed overview, we refer the reader to [14, Sec. 2]. The goal of the algorithm is to determine a map

$$\{x_j\}_{j=1}^n \subset \mathbb{R}^{d_1} \longrightarrow \{y_j\}_{j=1}^n \subset \mathbb{R}^{d_2} \tag{2.1}$$

with  $d_1 > d_2$ . By interpreting each data set as the discretization of a smooth Riemannian manifold, the algorithm was theoretically justified on compact manifolds without boundary in 2017 [8, 14] and on compact manifolds with boundary in 2023 [15]. Under this Riemannian manifold model, LLE unfolds a manifold locally to recover a global manifold embedded in a lower dimension. The local unfolding relies on parametrizing each data point as a linear combination of neighboring points and is encoded in a matrix  $W \in \mathbb{R}^{n \times n}$  known as the LLE matrix.

Given  $\{x_j\}_{j=1}^n$  sampled from a compact manifold embedded in  $\mathbb{R}^{d_1}$ , one can construct the LLE matrix directly. The matrix is designed to capture the local geometry of a high-dimensional data set; its entries are preserved during the lower-dimensional embedding. The algorithm begins with a choice of nearest-neighbor scheme. Typically, one specifies a small, positive parameter  $\epsilon$  and builds a neighborhood  $N_\epsilon(x_j)$  about each  $x_j$  that consists of all points  $x_i \neq x_j$  such that

$$\|x_i - x_j\|_{\ell^2(\mathbb{R}^{d_1})} < \epsilon.$$

However, we demonstrate the construction under the  $k$ -nearest neighbors scheme, which is numerically equivalent [14, Sec. 5]. For a given  $k \in \mathbb{N}$ , we build a neighborhood  $N_k(x_j)$  about each  $x_j$  that consists of the  $k$  closest data points, measured with the Euclidean metric on  $\mathbb{R}^{d_1}$ . In an effort to write each  $x_j$  as an affine combination of its neighbors, we then minimize

$$\sum_{j=1}^n \left\| x_j - \sum_{x_i \in N_k(x_j)} w_{ij} x_i \right\|_{\ell^2(\mathbb{R}^{d_1})}^2 \quad (2.2)$$

over all possible weights  $w_{ij} \in \mathbb{R}$  subject to the linear constraint

$$\sum_i w_{ij} = 1. \quad (2.3)$$

Interpreting  $w_{ij} = 0$  for  $x_i \notin N_k(x_j)$ , the barycentric coordinates  $w_{ij}$  form the elements of the sparse matrix  $W$ . In practice, this step is explicit; one can construct local data matrices  $G_j \in \mathbb{R}^{d_1 \times k}$  with columns given by the tangent vectors  $x_i - x_j$  for  $x_i \in N_k(x_j)$ . The minimization of (2.2) is then equivalent to minimizing the quadratic form  $w^T G_j^T G_j w$  under the same linear constraint in (2.3).

In general, the matrix  $G_j^T G_j$  need not be invertible, meaning the algorithm needs to be stabilized. This can be done by introducing the regularizer  $c > 0$  and solving

$$(G_j^T G_j + cI_{k \times k}) z_j = \mathbf{1}_k$$

where  $\mathbf{1}_k$  is a  $k \times 1$  vector with all entries equal to one. The weights then satisfy

$$w_{ij} = (z_j^T \mathbf{1}_k)^{-1} z_{ij}$$

where  $z_{ij}$  is the  $i$ th element of  $z_j$ . This regularizer plays a crucial role in the asymptotics of LLE, as discussed in [14]. In [15], Wu and Wu set

$$c = n\epsilon^{d_1+3} \quad (2.4)$$

where  $n$  is the number of data points and  $\epsilon$  is the neighborhood size. To ensure (1.2) holds, we retain this choice throughout.

The matrix  $W \in \mathbb{R}^{n \times n}$  has several key properties. It satisfies  $W\mathbf{1}_n = \mathbf{1}_n$  for all  $n$  and has a spectral radius no less than 1. It also becomes real and symmetric in the dimensional limit, as  $n$  increases [15, Prop. 2]. Once  $W$  is constructed, the bottom eigenvalues of the symmetric matrix  $(I - W)^T(I - W)$  then provide the embedding coordinates for the low-dimensional data set  $\{y_j\}_{j=1}^n$ . When  $n$  is large, this final step of the algorithm is computationally expensive, but  $W$  is well-approximated by  $D_\epsilon$  per (1.2).

### 3. LLE ON THE INTERVAL

In this section, we study eigenpairs  $(\lambda, u)$  satisfying (1.3) on the unit interval  $[0, 1]$ . As introduced in [15, Sec. 5], the differential operator  $D_\epsilon$  is a second order differential operator with piecewise coefficients. First, we derive the Sturm-Liouville form and use the Frobenius method to understand the pointwise behavior of the eigenfunctions. We show that taking  $u \in C^2([0, 1])$  is equivalent to imposing quasi-Neumann boundary conditions on the eigenfunctions of  $D_\epsilon$ . Then we use the eigenfunction regularity to determine an eigenvalue

condition. Finally, we discuss how to interpret the limiting eigenvalues variationally and prove Theorem 1.3 on the interval.

**3.1. Presentation of the differential operator on the interval.** While an exact definition of  $D_\epsilon$  on the unit interval  $M = [0, 1]$  is featured in [15, Cor. 17], we reproduce its form here for convenience. The boundary layer can be written  $M_\epsilon = [0, \epsilon] \cup (1 - \epsilon, 1]$  with Fermi coordinates

$$\begin{cases} x, & x \in [0, \epsilon) \\ 1 - x, & x \in (1 - \epsilon, 1]. \end{cases}$$

Due to this symmetry, we can globally define  $D_\epsilon$  on  $[0, 1]$  using [15, Def. 12] in the form

$$D_\epsilon f(x) = \phi_2(x)f''(x) + \phi_1(x)f'(x) \quad (3.1)$$

for  $f \in C^2([0, 1])$ . Here each coefficient  $\phi_1, \phi_2$  is constant outside the boundary layer. Namely,

$$D_\epsilon f(x) = -\frac{1}{6}\Delta f(x)$$

when  $x \in M \setminus M_\epsilon$ . In the boundary layer, both coefficients are real-analytic and uniformly bounded. The leading coefficient can be written

$$\phi_2(x) = \begin{cases} \frac{1}{12} \left( 1 - 4 \left( \frac{x}{\epsilon} \right) + \left( \frac{x}{\epsilon} \right)^2 \right), & \text{if } x \in [0, \epsilon]; \\ -\frac{1}{6}, & \text{if } x \in [\epsilon, 1 - \epsilon]; \\ \frac{1}{12} \left( 1 - 4 \left( \frac{1-x}{\epsilon} \right) + \left( \frac{1-x}{\epsilon} \right)^2 \right), & \text{if } x \in [1 - \epsilon, 1]. \end{cases}$$

Note that  $\phi_2$  is continuous on  $[0, 1]$ , symmetric across the midpoint  $x = \frac{1}{2}$ , and vanishes near the boundary. If we set

$$x_0 = (2 - \sqrt{3})\epsilon,$$

then  $D_\epsilon$  degenerates to a first order operator on  $\{x_0, 1 - x_0\}$ . These singularities demand a careful analysis and motivate our derivation of the Sturm-Liouville form in (3.2). The remaining coefficient in (3.1) can be written

$$\phi_1(x) = \begin{cases} -6 \left( 1 - \frac{x}{\epsilon} \right) \left( 1 + \frac{x}{\epsilon} \right)^{-3}, & \text{if } x \in [0, \epsilon]; \\ 0, & \text{if } x \in [\epsilon, 1 - \epsilon]; \\ 6 \left( 1 - \frac{1-x}{\epsilon} \right) \left( 1 + \frac{1-x}{\epsilon} \right)^{-3}, & \text{if } x \in [1 - \epsilon, 1]. \end{cases}$$

Similarly,  $\phi_1$  is continuous on  $[0, 1]$  and has an odd symmetry across the midpoint  $x = \frac{1}{2}$ . To rewrite (1.3) in divergence form, we construct an integration factor via the function

$$g(x) := \operatorname{sgn}(x - x_0) |x - x_0|^{(4+2\sqrt{3})\epsilon} |x - 4\epsilon + x_0|^{(4-2\sqrt{3})\epsilon} (x + \epsilon)^{-8\epsilon} e^{\frac{12\epsilon^3}{(\epsilon+x)^2} + \frac{12\epsilon^2}{\epsilon+x}}$$

defined for  $x \in [0, \epsilon]$ . If we set

$$p(x) = \begin{cases} \frac{g(x)}{6g(\epsilon)}, & \text{if } x \in [0, \epsilon]; \\ \frac{1}{6}, & \text{if } x \in [\epsilon, 1 - \epsilon]; \\ \frac{g(1-x)}{6g(\epsilon)}, & \text{if } x \in [1 - \epsilon, 1] \end{cases} \quad \text{and} \quad w(x) = -\frac{p(x)}{\phi_2(x)}$$

then (1.3) can be written as the differential equation

$$-(p(x)u'(x))' = \lambda w(x)u(x) \quad (3.2)$$



almost everywhere on  $[0, 1]$ . In particular, (3.2) is a regular Sturm-Liouville equation<sup>1</sup>, with coefficient properties detailed in the following statement.

**Proposition 3.1.** *For small enough  $\epsilon$ , the principal coefficient  $p$  satisfies the following properties:*

1.  $p(x)$  is continuous and  $\frac{1}{p}(x)$  is in  $L^1([0, 1])$ .
2.  $p(x)$  is positive for  $x \in (x_0, 1 - x_0)$ , negative for  $x \in [0, x_0) \cup (1 - x_0, 1]$ , and zero when  $x = x_0$  or  $x = 1 - x_0$ .
3.  $p(x)$  is asymptotic to  $\text{sgn}(x - x_0) |x - x_0|^{(4+2\sqrt{3})\epsilon}$  as  $x \rightarrow x_0$ .

The weight function  $w$  satisfies the following properties:

1.  $w(x)$  is continuous except at  $x_0, 1 - x_0$  and in  $L^1([0, 1])$ .
2.  $w(x)$  is positive for all  $x \in [0, 1]$ .
3.  $w(x) \rightarrow \infty$  as  $x \rightarrow x_0$  or  $x \rightarrow 1 - x_0$ .

For all  $x \in (0, 1)$ ,  $p(x)$  converges pointwise to  $\frac{1}{6}$  and  $w(x)$  converges pointwise to 1 as  $\epsilon \rightarrow 0$ .

The changing sign of  $p$  means that  $D_\epsilon$  is mixed-type. Under (1.5), (3.1) and Proposition 3.1, we identify the elliptic region as the set  $M_+ = \{x \in [0, 1] : p(x) > 0\}$  and the collection of interior singularities  $\Gamma = \{x_0, 1 - x_0\}$  as the interface between elliptic and hyperbolic regions. With the differential operator  $D_\epsilon$  constructed, we next establish properties of the eigenfunctions.

**3.2. Proof of Theorem 1.1.** In this section, we use the Frobenius method to study eigenfunctions of the differential operator presented in the previous section and prove Theorem 1.1. The regularity condition  $u \in C^2([0, 1])$  identifies a unique solution to (3.2) in the boundary layer, and matching conditions with the interior provide an exact eigenvalue condition. More precisely, if we define

$$u_L(x) = u(x)|_{[0, \epsilon]}, \quad u_M(x) = u(x)|_{[\epsilon, 1 - \epsilon]}, \quad \text{and} \quad u_R(x) = u(x)|_{[1 - \epsilon, 1]},$$

then (3.2) can be solved on each subinterval, and a global solution can be determined by gluing local solutions together. By symmetry of (3.1),  $u_L(x)$  and  $u_R(1 - x)$  are linearly dependent, so we begin our analysis near the left boundary, where (3.2) admits two local, linearly-independent solutions. Because the coefficients in (3.1) are analytic over their respective domains, these solutions can be written as a Frobenius series centered at the singularity. The following result describes possible solution behavior in the leftmost boundary layer.

**Proposition 3.2.** *Let  $(\lambda, u)$  satisfy (3.2) on the unit interval. The local solution  $u_L(x) = u(x)|_{[0, \epsilon]}$  is a linear combination of two functions that we denote as  $u_{\text{Dir}}$  and  $u_{\text{Neu}}$ . The solution  $u_{\text{Dir}}$  satisfies*

$$u_{\text{Dir}}(x_0) = 0 \quad \text{and} \quad \lim_{x \rightarrow x_0} p(x)u'_{\text{Dir}}(x) = 1$$

while the solution  $u_{\text{Neu}}$  satisfies

$$u_{\text{Neu}}(x_0) = 1 \quad \text{and} \quad \lim_{x \rightarrow x_0} p(x)u'_{\text{Neu}}(x) = 0.$$

In particular,  $u_{\text{Dir}}$  is continuous but not  $C^1(0, \epsilon)$  while  $u_{\text{Neu}}$  is  $C^\infty(0, \epsilon)$ .

The notation for each basis function stems from their behavior at the singularity  $x_0$ . In Proposition 3.3 below, we include estimates for both functions, although the condition  $u \in C^2([0, 1])$  discards any contribution from  $u_{\text{Dir}}$ . Thus, the left solution  $u_L$  is precisely the Neumann solution.

---

<sup>1</sup>If we apply a global sign change to  $\phi_1(x)$ , then (3.2) is a singular Sturm-Liouville equation, which enforces a Dirichlet boundary condition on the elliptic region.

*Proof of Proposition 3.2.* The variable coefficients in (3.1) are analytic and have a series representation centered at  $x_0$ . We write

$$\phi_2(x) = \sum_{j=1}^2 a_j (x - x_0)^j \quad \text{with} \quad a_1 = -\frac{1}{\sqrt{12}\epsilon} \quad \text{and} \quad a_2 = \frac{1}{12\epsilon^2}$$

and

$$\phi_1(x) = \sum_{j=0}^{\infty} b_j (x - x_0)^j \quad \text{with} \quad b_j = 6 \frac{(-1)^{j+1}}{\epsilon^j} \left( \frac{j^2 + \sqrt{3}j + \sqrt{3} - 1}{(3 - \sqrt{3})^{j+3}} \right)$$

for all  $j \geq 0$ . Any local solution on  $(0, \epsilon)$  takes the form of a Frobenius series

$$u(x) = \sum_{j=0}^{\infty} c_j (x - x_0)^{j+\alpha} \tag{3.3}$$

for  $\alpha \in \mathbb{R}$ . The indicial polynomial

$$P(\alpha) = a_1 \alpha(\alpha - 1) + b_0 \alpha \tag{3.4}$$

has two roots at 0 and  $1 - (4 + 2\sqrt{3})\epsilon$ . Because these roots differ by a non-integer for small enough  $\epsilon$ , there are two linearly independent solutions to (3.2) near the left boundary, each with series given by (3.3). Without loss of generality, we initially take  $c_0 = 1$  for both solutions. For  $j \geq 1$ , the remaining Frobenius coefficients can be determined through the recurrence relation

$$P(\alpha + j)c_j = (\lambda - a_2(\alpha + j - 1)(\alpha + j - 2))c_{j-1} - \sum_{k=0}^{j-1} c_k(k + \alpha)b_{j-k}. \tag{3.5}$$

When  $\alpha = 1 - (4 + 2\sqrt{3})\epsilon$ , we denote the series (3.3) as the Dirichlet solution so that  $u_{\text{Dir}}(x_0) = 0$ . Proposition 3.1 then implies that the quasi-derivative  $p_1(x)u'_{\text{Dir}}(x)$  has a finite, nonzero limit as  $x$  approaches  $x_0$ . When  $\alpha = 0$ , we denote the series (3.3) as the Neumann solution so that  $p_1(x_0)u'_{\text{Neu}}(x_0) = 0$ . By scaling both solutions appropriately, we have the desired result.  $\square$

Proposition 3.2 implies that the regularity condition  $u \in C^2([0, 1])$  is equivalent to imposing quasi-Neumann boundary conditions on the elliptic region  $M_+$ . This necessarily means that the spectrum is discrete [9, Ch. 5], and the eigenvalues of  $D_\epsilon$  can be written as

$$\lambda = \frac{\int_{x_0}^{1-x_0} p(x) |u'(x)|^2 dx}{\int_{x_0}^{1-x_0} w(x) |u(x)|^2 dx} \tag{3.6}$$

for  $u$  satisfying (3.2). By Proposition 3.1 alongside (3.6), the eigenvalues are real and nonnegative and the eigenfunctions are orthogonal with respect to the  $L^2(M_+, w)$  inner product. Because  $w(x)$  converges pointwise to 1 as  $\epsilon \rightarrow 0$ , this corresponds to the fact that the LLE matrix is symmetric and real in the dimensional limit. Further, when  $\lambda = 0$ , the remaining Neumann solution  $u_{\text{Neu}}$  is a constant. By (1.2), this verifies that constant vectors are eigenvectors of the LLE matrix and completes the proof of Theorem 1.1.

To estimate eigenvalues via (3.6) would require a complete understanding of the related eigenfunctions over the elliptic region. Because  $D_\epsilon$  is defined piecewise in (3.1), we can alternatively characterize the eigenvalues by the continuity conditions imposed at  $\epsilon$  and  $1 - \epsilon$ . The following estimates follow from the proof of Proposition 3.2.

**Proposition 3.3.** *Let  $(\lambda, u)$  satisfy (3.2) on  $[0, 1]$  with*

$$\lim_{\epsilon \rightarrow 0} |\lambda(\epsilon)|\epsilon^2 = 0.$$

There exist constants  $C$  and  $\epsilon_0$  such that if  $0 < \epsilon \leq \epsilon_0$ , then  $u_{\text{Dir}}$  satisfies

$$|u_{\text{Dir}}(\epsilon)| \leq C\epsilon \quad \text{and} \quad |u'_{\text{Dir}}(\epsilon) - 1| \leq C\epsilon(1 + \epsilon|\lambda|)$$

and  $u_{\text{Neu}}$  satisfies

$$|u_{\text{Neu}}(\epsilon) - 1| \leq C\epsilon|\lambda| \quad \text{and} \quad |u'_{\text{Neu}}(\epsilon) - (3 - 2\sqrt{3})\lambda| \leq C\epsilon|\lambda|(1 + \epsilon|\lambda|).$$

Because (3.2) has a spectral parameter, the coefficients in (3.3) depend explicitly on the eigenvalue; the condition on  $\lambda$  avoids complications from this dependence. Additionally, the terms in the respective series for  $u_{\text{Dir}}$  and  $u_{\text{Neu}}$  lose any sense of ordering with respect to  $\epsilon$  for  $|\lambda|$  comparable to  $\epsilon^{-2}$ . Because LLE utilizes only the smallest eigenvalues in the spectrum, as indicated in Section 2, this condition is justifiable.

*Proof of Proposition 3.3.* By taking  $|\lambda|\epsilon^2 \rightarrow 0$  as  $\epsilon \rightarrow 0$ , we ensure that the constants in Proposition 3.3 are independent of the eigenvalue. As in Proposition 3.2, there are two solutions to consider, each corresponding to a different root of the indicial polynomial (3.4). Retaining the notation from the proof of Proposition 3.2, there exists a constant  $C$  such that

$$|b_j| \leq Cj^{-1}\epsilon^{-j} \tag{3.7}$$

for all  $j \geq 1$ . We break this proof into two cases depending on the root  $\alpha$ .

**Case 1.** Consider  $u_{\text{Dir}}$  when  $\alpha = 1 - (4 + 2\sqrt{3})\epsilon$ . The first coefficient  $c_1$  is bounded by a multiple of  $1 + \epsilon|\lambda|$ , and because  $|\lambda|\epsilon^2 = o(1)$ , (3.5) and (3.7) inductively imply that

$$|c_j| \leq \epsilon^{1-j}|c_1|$$

for all  $j \geq 1$ . We expand

$$u_{\text{Dir}}(\epsilon) = (\epsilon - x_0)^{1-(4+2\sqrt{3})\epsilon} + (\epsilon - x_0)^{1-(4+2\sqrt{3})\epsilon} \sum_{j=1}^{\infty} c_j(\epsilon - x_0)^j,$$

noting that the first term above is bounded by a multiple of  $\epsilon$  and the second term can be bounded

$$\left| (\epsilon - x_0)^{1-(4+2\sqrt{3})\epsilon} \sum_{j=1}^{\infty} c_j(\epsilon - x_0)^j \right| \leq C\epsilon^2|c_1| \sum_{j=1}^{\infty} \left| 1 - \frac{x_0}{\epsilon} \right|^j. \tag{3.8}$$

Because  $\left| 1 - \frac{x_0}{\epsilon} \right| < 1$ , (3.8) features a convergent geometric series and is bounded by a multiple of  $\epsilon^2(1 + \epsilon|\lambda|)$ . Again because  $|\lambda|\epsilon^2 = o(1)$ , this provides the pointwise bound for  $u_{\text{Dir}}$ . The derivative estimate holds similarly.

**Case 2.** Consider  $u_{\text{Neu}}$  when  $\alpha = 0$ . The first coefficient  $c_1$  is equal to  $(3 - 2\sqrt{3})\lambda$ , but we need to consider coefficients of higher indices. The second coefficient  $c_2$  is bounded by a multiple of  $|\lambda|(1 + \epsilon|\lambda|)$  and because  $\lambda\epsilon^2 = o(1)$ , (3.5) and (3.7) inductively imply that

$$|c_j| \leq \epsilon^{2-j}|c_2|$$

for all  $j \geq 2$ . We expand

$$u_{\text{Neu}}(\epsilon) = 1 + c_1(\epsilon - x_0) + \sum_{j=2}^{\infty} c_j(\epsilon - x_0)^j,$$

noting that the second term above is bounded by a multiple of  $\epsilon|\lambda|$  and the third term can be bounded

$$\left| \sum_{j=2}^{\infty} c_j(\epsilon - x_0)^j \right| \leq C\epsilon^2|c_2| \sum_{j=2}^{\infty} \left| 1 - \frac{x_0}{\epsilon} \right|^j. \tag{3.9}$$

As in the previous case, the geometric series is convergent and (3.9) is bounded by a multiple of  $\epsilon^2|\lambda|(1 + \epsilon|\lambda|)$ . Because  $|\lambda|\epsilon^2 = o(1)$ , this provides the pointwise bound for  $u_{\text{Neu}}$ . The derivative estimate holds similarly.  $\square$

Because we require the eigenfunctions to be sufficiently regular, the spectral behavior of  $D_\epsilon$  can be estimated via matching conditions and eigenfunction estimates. This results in the following statement, which identifies eigenvalues as roots of an explicit transcendental equation.

**Proposition 3.4.** *Let  $(\lambda, u) \in [0, \infty) \times C^2([0, 1])$  satisfy (3.2). If  $u_L(x) = u(x)|_{[0, \epsilon]}$  and  $\epsilon$  is sufficiently small, then the eigenvalue  $\lambda$  satisfies*

$$\sin\left(\sqrt{6\lambda}(1-2\epsilon)\right)\left(u_L'^2(\epsilon) - 6\lambda u_L^2(\epsilon)\right) + 2\sqrt{6\lambda}\cos\left(\sqrt{6\lambda}(1-2\epsilon)\right)\left(u_L(\epsilon)u_L'(\epsilon)\right) = 0.$$

This result effectively describes the process of gluing local solutions to form a global eigenfunction. The regularity condition not only isolates a unique solution in the boundary layer, as highlighted in Proposition 3.2, but it also enforces this matching condition.

*Proof of Proposition 3.4.* Because  $u \in C^2([0, 1])$ , the eigenvalue  $\lambda$  must simultaneously verify

$$\lim_{x \rightarrow \epsilon^-} u_L(x) = \lim_{x \rightarrow \epsilon^+} u_M(x) \quad \text{and} \quad \lim_{x \rightarrow \epsilon^-} u_L'(x) = \lim_{x \rightarrow \epsilon^+} u_M'(x)$$

along with

$$\lim_{x \rightarrow \epsilon^-} u_M(x) = \lim_{x \rightarrow \epsilon^+} u_R(x) \quad \text{and} \quad \lim_{x \rightarrow \epsilon^-} u_M'(x) = \lim_{x \rightarrow \epsilon^+} u_R'(x).$$

Note that by (3.1), these two conditions guarantee continuity of the second derivative at  $\epsilon$ . The local solution  $u_M$  is a Laplacian eigenfunction with frequency  $\sqrt{6\lambda}$ , i.e. a linear combination of sines and cosines. For  $u$  to be nontrivial, the following matrix

$$\begin{pmatrix} u_L(\epsilon) & 0 & -1 & 0 \\ 0 & -\sin\left(\sqrt{6\lambda}(1-2\epsilon)\right) & -\cos\left(\sqrt{6\lambda}(1-2\epsilon)\right) & u_L(\epsilon) \\ u_L'(\epsilon) & -\sqrt{6\lambda} & 0 & 0 \\ 0 & -\sqrt{6\lambda}\cos\left(\sqrt{6\lambda}(1-2\epsilon)\right) & \sqrt{6\lambda}\sin\left(\sqrt{6\lambda}(1-2\epsilon)\right) & -u_L'(\epsilon) \end{pmatrix}$$

must have zero determinant. This condition equates eigenvalues to roots of the desired transcendental equation.  $\square$

In combination, Proposition 3.3 and Proposition 3.4 prove the following first order estimate for the eigenvalues of  $D_\epsilon$  on the interval.

**Corollary 3.5.** *Let  $u \in C^2([0, 1])$  satisfy (1.3) on  $[0, 1]$  with eigenvalue  $\lambda = \lambda(\epsilon)$ . If  $\lim_{\epsilon \rightarrow 0} |\lambda|\epsilon^2 = 0$ , then there exist positive constants  $C, \epsilon_0$  such that for all  $0 < \epsilon \leq \epsilon_0$ ,*

$$\left| \sin\left(\sqrt{6\lambda}\right) \left( (21 - 12\sqrt{3})\lambda - 6 \right) + 2\sqrt{6\lambda} \left( 3 - 2\sqrt{3} \right) \cos\left(\sqrt{6\lambda}\right) \right| \leq C\epsilon |\lambda|^{\frac{3}{2}}.$$

By taking  $\lambda(\epsilon)$  smaller than  $\epsilon^{-\rho}$  for any  $\rho < \frac{2}{3}$  and letting  $\epsilon$  vanish, we close the bootstrapping argument and recover a complete description of the eigenvalues of the limiting operator. Note that the error increases further in the spectrum. The eigenvalues also share a variational interpretation under the requirement that each eigenfunction be  $C^2([0, 1])$ . If we define the energy functional

$$E(f) = \frac{\int_{x_0}^{1-x_0} p(x) |f'(x)|^2 dx}{\int_{x_0}^{1-x_0} w(x) |f(x)|^2 dx} \quad (3.10)$$

over all  $f$  for which  $E(f)$  is finite, then the minimizers of  $E$  on orthogonal subspaces of  $L^2(M_+, w)$  are eigenfunctions of (3.2) with Neumann boundary conditions [3, Ch. 6] in the sense that

$$\lim_{x \rightarrow x_0} p(x)f'(x) = 0.$$

In this manner, the eigenvalues satisfy an infinite-dimensional min-max principle analogous to the Rayleigh min-max principle for matrices. This proves Theorem 1.3 on the interval.

**Remark 3.6.** In [15, Sec. 7], Wu and Wu introduce the clipped LLE matrix, a useful tool for numerically estimating eigenfunctions of the Dirichlet Laplacian on manifolds in which the elliptic region (1.5) is known a priori. By Proposition 3.2, this corresponds directly to setting  $u_L(x) = u_{\text{Dir}}(x)$  in the left boundary layer. In combination, Propositions 3.3 and 3.4 provide estimates for eigenvalue convergence of the clipped LLE matrix.

#### 4. LLE ON THE DISC

In this section, we study eigenpairs  $(\lambda, u)$  satisfying (1.3) on the unit disc  $M = \overline{B_1(0)}$ . First, we present an explicit expression for  $D_\epsilon$  on the disc and find its Sturm-Liouville form. Following the same argument as in Section 3, we then isolate a unique eigenfunction in the boundary layer and use regularity to determine an exact eigenvalue condition. Finally, we prove Theorem 1.2 and present the eigenvalues in a variational format.

**4.1. Presentation of the differential operator on the disc.** In this section, we use [15, Def. 12] to explicitly derive the differential operator  $D_\epsilon$  on the unit disc. The boundary layer can be written

$$M_\epsilon = \{(r, \theta) : 1 - \epsilon < r \leq 1\}$$

with Fermi polar coordinates  $(1 - r, \theta)$ . Due to the radial symmetry, there exist differential operators  $\partial_{11}^2, \partial_{22}^2, \partial_2$  such that  $D_\epsilon$  can be globally defined on the disc with the form

$$D_\epsilon f(r, \theta) = \phi_{11}(1 - r)\partial_{11}^2 f(r, \theta) + \phi_{22}(1 - r)\partial_{22}^2 f(r, \theta) + \phi_2(1 - r)\partial_2 f(r, \theta) \quad (4.1)$$

for  $f \in C^2(\overline{B_1(0)})$ . The variable coefficients in (4.1) are defined in terms of sigma functions that capture the geometric asymmetries of a neighborhood of each point. Each coefficient is constant outside the boundary layer, reducing to

$$D_\epsilon f(x) = -\frac{1}{8}\Delta f(x)$$

for  $x \in M \setminus M_\epsilon$ .

We can write the leading order coefficients as

$$\begin{aligned} \phi_{11}(t) &= \frac{1}{2} \frac{\sigma_{2,2}(t)\sigma_2(t) - \sigma_3(t)\sigma_{1,2}(t)}{\sigma_{1,2}^2(t) - \sigma_{2,2}(t)\sigma_0(t)} \\ \phi_{22}(t) &= \frac{1}{2} \frac{\sigma_{2,2}^2(t) - \sigma_{3,2}(t)\sigma_{1,2}(t)}{\sigma_{1,2}^2(t) - \sigma_{2,2}(t)\sigma_0(t)} \end{aligned}$$

and the remaining coefficient as

$$\phi_2(t) = \frac{\sigma_{1,2}(t)}{\sigma_{1,2}^2(t) - \sigma_{2,2}(t)\sigma_0(t)}.$$

The sigma functions can be derived explicitly for a given dimension and have a common geometric interpretation, as discussed in [15, Def. 7]. In dimension 2, they are defined as follows:

$$\begin{aligned} \sigma_0(t) &= \begin{cases} \frac{\pi}{2} + \frac{t}{\epsilon} \sqrt{1 - \left(\frac{t}{\epsilon}\right)^2} + \arcsin\left(\frac{t}{\epsilon}\right), & 0 \leq t \leq \epsilon \\ \pi, & \text{otherwise} \end{cases} \\ \sigma_{1,2}(t) &= \begin{cases} -\frac{2}{3} \left(1 - \left(\frac{t}{\epsilon}\right)^2\right)^{\frac{3}{2}}, & 0 \leq t \leq \epsilon \\ 0, & \text{otherwise} \end{cases} \end{aligned}$$

$$\begin{aligned}
\sigma_2(t) &= \begin{cases} \frac{\pi}{8} + \frac{1}{12} \left( \frac{t}{\epsilon} \sqrt{1 - \left(\frac{t}{\epsilon}\right)^2} \left(5 - 2 \left(\frac{t}{\epsilon}\right)^2\right) + 3 \arcsin \left(\frac{t}{\epsilon}\right) \right), & 0 \leq t \leq \epsilon \\ \frac{\pi}{4}, & \text{otherwise} \end{cases} \\
\sigma_{2,2}(t) &= \begin{cases} \frac{\pi}{8} + \frac{1}{4} \left( \frac{t}{\epsilon} \sqrt{1 - \left(\frac{t}{\epsilon}\right)^2} \left(2 \left(\frac{t}{\epsilon}\right)^2 - 1\right) + \arcsin \left(\frac{t}{\epsilon}\right) \right), & 0 \leq t \leq \epsilon \\ \frac{\pi}{4}, & \text{otherwise} \end{cases} \\
\sigma_3(t) &= \begin{cases} -\frac{2}{15} \left(1 - \left(\frac{t}{\epsilon}\right)^2\right)^{\frac{5}{2}}, & 0 \leq t \leq \epsilon \\ 0, & \text{otherwise} \end{cases} \\
\sigma_{3,2}(t) &= \begin{cases} -\frac{2}{15} \left(2 + 3 \left(\frac{t}{\epsilon}\right)^2\right) \left(1 - \left(\frac{t}{\epsilon}\right)^2\right)^{\frac{3}{2}}, & 0 \leq t \leq \epsilon \\ 0, & \text{otherwise.} \end{cases}
\end{aligned} \tag{4.2}$$

Notice that each sigma function above is analytic on  $(0, \epsilon)$  but cannot extend analytically beyond  $t = \epsilon$ . This contrasts the leading coefficient of  $D_\epsilon$  on the interval, as presented in Section 3. While these sigma functions are crucial for the numerical analysis in Section 5, we only use a few key properties in this section. The following statement follows directly from (4.2) and [15, Prop. 13].

**Proposition 4.1.** *For small enough  $\epsilon$ , the variable coefficients in (4.1) have the following properties.*

1.  $\phi_{11}(t)$  is negative for all  $t \geq 0$  and  $\phi_{11}(t) = -\frac{1}{8}$  for  $t \geq \epsilon$ .
2.  $\phi_{22}(t) = -\frac{1}{8}$  for  $t \geq \epsilon$ .
3.  $\phi_{22}(0) > 0$  and there exists a unique  $r_0 \in (0, \epsilon)$  such that  $\phi_{22}(r_0) = 0$ .
4.  $\phi_{22}(t)$  vanishes linearly at  $r_0$ , in the sense that  $\phi'_{22}(r_0) \neq 0$ .
5.  $\phi_2(t)$  is nonnegative for all  $t \geq 0$  and  $\phi_2(t) = 0$  for  $t \geq \epsilon$ .

Additionally, each coefficient is continuous and uniformly bounded on  $[0, 1]$  and analytic except at  $t = \epsilon$ .

Although each function in Proposition 4.1 can be written explicitly using (4.2), the featured properties are sufficient for proving Theorem 1.2. Because  $\phi_{22}(1 - r)$  vanishes in the boundary layer, the elliptic and hyperbolic regions (1.5) are separated by a circle of radius  $1 - r_0$ , where  $r_0$  is the unique root of  $\phi_{22}$ .

To present  $D_\epsilon$  in its entirety, we lastly need to present the differential operators  $\partial_{11}^2, \partial_{22}^2, \partial_2$  in (4.1). We define

$$\partial_{11}^2 = \frac{1}{r} \frac{\partial}{\partial r} + \frac{1}{r^2} \frac{\partial^2}{\partial \theta^2}, \quad \partial_{22}^2 = \frac{\partial^2}{\partial r^2}, \quad \text{and} \quad \partial_2 = \frac{\partial}{\partial r} \tag{4.3}$$

so that (4.1) verifies the pointwise construction featured in [15, Def. 12]. Namely, for a fixed  $x$  in the boundary layer,

$$\partial_i f(x) = \frac{d}{dt} (f \circ \gamma_i)(0)$$

where  $\gamma_i(t)$  is a geodesic satisfying  $\gamma_i(0) = x$ . In particular,  $\partial_{11}^2 + \partial_{22}^2$  is the polar Laplacian and  $\partial_2$  is oriented towards the boundary. Equations (4.2) and (4.3) provide the polar representation of  $D_\epsilon$ .

The fact that  $D_\epsilon$  degenerates follows from the properties of  $\phi_{22}$  in Proposition 4.1 and is more clear by writing (1.3) in the separable Sturm-Liouville form

$$-\frac{\partial}{\partial r} \left( p(1-r) \frac{\partial u}{\partial r}(r, \theta) \right) + q(1-r) \frac{\partial^2 u}{\partial \theta^2}(r, \theta) = \lambda w(1-r) u(r, \theta). \tag{4.4}$$

Here the principal coefficient  $p$  is defined as

$$p(1-r) = \frac{1}{8} (1-\epsilon) \operatorname{sgn}(1-r_0-r) \exp \left( \int_{1-\epsilon}^r \frac{\phi_{11}(1-s) + s\phi_2(1-s)}{s\phi_{22}(1-s)} ds \right) \tag{4.5}$$

which is sign-changing and vanishes when  $r = 1 - r_0$ . The remaining coefficients are defined as

$$q(1-r) = -\frac{p(1-r)}{r^2} \left( \frac{\phi_{11}(1-r)}{\phi_{22}(1-r)} \right)$$

$$w(1-r) = -\frac{p(1-r)}{\phi_{22}(1-r)}.$$

The prefactor in (4.5) is chosen so that the weight  $w$  is equal to  $r$  outside the boundary layer. Note that (4.4) is not necessary for the numerical comparison in Section 5, but it helps establish the variational interpretation of the eigenvalues. The following statement provides a few key details regarding these coefficients.

**Proposition 4.2.** *For small enough  $\epsilon$ , the Sturm-Liouville coefficients have the following properties. The principal coefficient  $p$  satisfies:*

1.  $p(1-r)$  is continuous and  $\frac{1}{p}(1-r)$  is in  $L^1(\delta, 1)$  for any  $\delta > 0$ .
2.  $p(1-r)$  is positive for  $r \in (0, 1-r_0)$ , negative for  $r \in (1-r_0, 1]$  and zero when  $r = 0$  or  $r = 1-r_0$ .
3.  $p(1-r)$  is asymptotic to  $\text{sgn}(1-r_0-r)(r-1+r_0)^\zeta$  as  $r \rightarrow 1-r_0$  with  $\zeta = \frac{\phi_{11}(r_0)+(1-r_0)\phi_2(r_0)}{(1-r_0)\phi'_{22}(r_0)}$ .

The coefficient  $q$  satisfies:

1.  $q(1-r)$  is continuous except at  $1-r_0$  and in  $L^1(\delta, 1)$  for any  $\delta > 0$ .
2.  $q(1-r)$  is negative for all  $r \in (0, 1)$ .
3.  $q(1-r) \rightarrow -\infty$  as  $r \rightarrow 1-r_0$ .

The weight  $w$  satisfies:

1.  $w(1-r)$  is continuous except at  $1-r_0$  and in  $L^1(0, 1)$ .
2.  $w(1-r)$  is positive for all  $r \in (0, 1)$ .
3.  $w(1-r) \rightarrow \infty$  as  $r \rightarrow 1-r_0$ .

For all  $r \in (0, 1)$ ,  $p(1-r)$  converges pointwise to  $\frac{r}{8}$ ,  $q(1-r)$  converges pointwise to  $-\frac{1}{8r}$ , and  $w(1-r)$  converges pointwise to  $r$  as  $\epsilon \rightarrow 0$ .

The changing sign of  $p$  means that  $D_\epsilon$  is mixed-type. Under (1.5), (4.4), and Proposition 4.2, we identify the elliptic region as the set  $M_+ = \{(r, \theta) : p(1-r) > 0\}$  and the singular surface  $\Gamma = \{(r, \theta) : r = 1-r_0\}$  as the interface between elliptic and hyperbolic regions. With a form for  $D_\epsilon$  established on the disc, we now prove Theorem 1.2 following the same argument as in Section 3.2.

**4.2. Proof of Theorem 1.2.** In this section, we use Proposition 4.1 and the polar representation of  $D_\epsilon$  to prove Theorem 1.2. As on the interval, we demonstrate how the Frobenius method determines the regularity of eigenfunctions in the boundary layer and provide a method for finding eigenvalues of  $D_\epsilon$  under the  $C^2$  regularity condition.

The coefficients in (4.1) are radial, meaning the eigenfunctions are necessarily separable. Supposing  $u$  satisfies (1.3) on the unit disc, we decompose the eigenfunction into radial and angular components

$$u(\theta, r) = u^\theta(\theta)u^r(r).$$

The eigenvalue equation (1.3) then reduces to a system of ordinary differential equations. The radial component  $u^r$  is determined by the equation

$$\phi_{22}(1-r)(u^r)''(r) + \left( \frac{1}{r}\phi_{11}(1-r) + \phi_2(1-r) \right) (u^r)'(r) - \frac{\nu^2}{r^2}\phi_{11}(1-r)u^r(r) = \lambda u^r(r) \quad (4.6)$$

while up to a phase shift, the angular component  $u^\theta$  is a multiple of  $\cos(\nu\theta)$ . For  $u$  to be continuous, we take  $\nu$  to be a nonnegative integer. Because the coefficients in (4.1) are defined piecewise in the radial coordinate, we decompose the radial eigenfunction  $u^r$  into an inner and outer solution. More precisely, if we set

$$u_I^r(r) = u^r(r)|_{[0,1-\epsilon]} \quad \text{and} \quad u_O^r(r) = u^r(r)|_{[1-\epsilon,1]},$$

then (4.6) can be solved on each subinterval, and a global solution can be determined by gluing local solutions together. Note that (4.4) is singular near the origin; this serves as an interior boundary condition, forcing the eigenfunction to vanish at the origin whenever  $\nu \neq 0$ . The inner solution can be solved explicitly, so we begin our analysis with the more complicated outer solution. In the boundary layer, there are two radial solutions to (4.6), each with a Frobenius series centered at the singularity  $1 - r_0$ . The following result is analogous to Proposition 3.2, describing the behavior of both local solutions near the edge of the boundary layer.

**Proposition 4.3.** *Let  $(\lambda, u)$  satisfy (4.4) on the unit disc. The local radial solution  $u_O^r(r) = u^r(r)|_{[1-\epsilon,1]}$  is a linear combination of two functions that we denote as  $u_{\text{Dir}}^r$  and  $u_{\text{Neu}}^r$ . The solution  $u_{\text{Dir}}^r$  satisfies*

$$u_{\text{Dir}}^r(1 - r_0) = 0 \quad \text{and} \quad \lim_{r \rightarrow 1-r_0} p(1-r)(u_{\text{Dir}}^r)'(r) = 1$$

while the solution  $u_{\text{Neu}}^r$  satisfies

$$u_{\text{Neu}}^r(1 - r_0) = 1 \quad \text{and} \quad \lim_{r \rightarrow 1-r_0} p(1-r)(u_{\text{Neu}}^r)'(r) = 0.$$

In particular,  $u_{\text{Dir}}^r$  is continuous but not  $C^1(1-\epsilon, 1)$  while  $u_{\text{Neu}}^r$  is  $C^\infty(1-\epsilon, 1)$ .

The notation for each basis function stems from their behavior at the singularity  $1 - r_0$ . The condition that  $u \in C^2(\overline{B_1(0)})$  discards any contribution from the Dirichlet solution, and therefore the outer solution  $u_O^r$  is precisely the Neumann solution.

*Proof of Proposition 4.3.* Under the transformation  $r \rightarrow 1 - r$ , we study (4.6) on  $[0, \epsilon]$ . Let  $r_0$  be the unique zero of  $\phi_{22}$  in this region, introduced in Proposition 4.1. Each variable coefficient in (4.6) is analytic on  $(0, \epsilon)$  and has a series representation centered at  $r_0$ . For the sake of notation, we write

$$\begin{aligned} \phi_{22}(r) &= \sum_{j=1}^{\infty} a_j (r - r_0)^j \\ \frac{1}{1-r} \phi_{11}(r) + \phi_2(r) &= \sum_{j=0}^{\infty} b_j (r - r_0)^j \\ \frac{1}{(1-r)^2} \phi_{11}(r) &= \sum_{j=0}^{\infty} d_j (r - r_0)^j \end{aligned}$$

where  $a_1, b_0$ , and  $d_0$  are all nonzero. By (4.2), each coefficient  $a_j, b_j, d_j$  scales with  $\epsilon^{-j}$ . Any local solution to (4.6) on  $(0, \epsilon)$  takes the form of a Frobenius series

$$u(1-r) = \sum_{j=0}^{\infty} c_j (r - r_0)^{j+\alpha} \tag{4.7}$$

for  $\alpha \in \mathbb{R}$ . The indicial polynomial

$$P(\alpha) = a_1 \alpha(\alpha - 1) + b_0 \alpha$$

has two roots at 0 and  $1 - \frac{b_0}{a_1}$ . By Proposition 4.1,  $\frac{b_0}{a_1}$  is bounded by a multiple of  $\epsilon$  and therefore these roots differ by a non-integer for small enough  $\epsilon$ . Hence there are two linearly independent solutions to (4.6) near



the boundary that take the form (4.7). Without loss of generality, we initially take  $c_0 = 1$  for both solutions. For  $j \geq 1$ , the remaining Frobenius coefficients can be determined through the recurrence relation

$$P(\alpha + j)c_j = \lambda c_{j-1} - \sum_{k=0}^{j-1} c_k \left( (k + \alpha)(k + \alpha - 1)a_{j-k+1} + (k + \alpha)b_{j-k} - \nu^2 d_{j-k-1} \right). \quad (4.8)$$

When  $\alpha = 1 - \frac{b_0}{a_1}$ , we denote the series (4.7) as the Dirichlet solution so that  $u_{\text{Dir}}^r(1 - r_0) = 0$ . Proposition 4.2 implies that the quasi-derivative  $p(1 - r)(u_{\text{Dir}}^r)'(r)$  has a finite, nonzero limit as  $r$  approaches  $1 - r_0$ . When  $\alpha = 0$ , we denote the series (4.7) as the Neumann solution so that  $p(r_0)(u_{\text{Neu}}^r)'(1 - r_0) = 0$ . By scaling both solutions appropriately, we have the desired result.  $\square$

Proposition 4.3 states that the regularity condition  $u \in C^2(\overline{B_1(0)})$  is equivalent to imposing quasi-Neumann boundary conditions on the elliptic region, just as in Section 3. Similarly, the spectrum of  $D_\epsilon$  then consists entirely of eigenvalues satisfying

$$\lambda = \frac{\int_0^{1-r_0} p(1-r) |(u^r)'(r)|^2 dr - \nu^2 \int_0^{1-r_0} q(1-r) |u^r(r)|^2 dr}{\int_0^{1-r_0} w(1-r) |u^r(r)|^2 dr} \quad (4.9)$$

for  $u^r$  satisfying (4.6). By Proposition 4.1 alongside (4.9), the eigenvalues are real and nonnegative and the eigenfunctions are orthogonal with respect to the  $L^2(M_+, w)$  inner product. Because  $w(1 - r)$  converges pointwise to  $r$  as  $\epsilon \rightarrow 0$ , this corresponds to the fact that the LLE matrix is symmetric and real in the dimensional limit. Further, when  $\nu = 0$ , (4.9) admits a zero eigenvalue, for which the Neumann solution  $u_{\text{Neu}}^r$  is a constant. By (1.2), this verifies that constant vectors are eigenvectors of the LLE matrix and completes the proof of Theorem 1.2.

As in Section 3, determining eigenvalues via (4.9) would prove difficult. Instead, we rely on the pointwise estimates in Proposition 4.3 and the continuity conditions at the boundary layer. This results in the following statement, which identifies eigenvalues as roots of a transcendental equation.

**Proposition 4.4.** *Let  $(\lambda, u) \in [0, \infty) \times C^2(\overline{B_1(0)})$  satisfy (4.4) with  $\nu \in \mathbb{N}_0$ . If  $u_O^r(r) = u^r(r)|_{[1-\epsilon, 1]}$  and  $\epsilon$  is sufficiently small, then the eigenvalue  $\lambda$  satisfies*

$$J_\nu \left( \sqrt{8\lambda}(1 - \epsilon) \right) (u_O^r)'(1 - \epsilon) - \sqrt{8\lambda} J'_\nu \left( \sqrt{8\lambda}(1 - \epsilon) \right) u_O^r(1 - \epsilon) = 0.$$

Here  $J_\nu$  denotes a Bessel function of the first kind.

This eigenvalue condition appears simpler than that presented in Proposition 3.4, when  $D_\epsilon$  is defined over the unit interval. This is because the boundary layer in the disc is connected, so there are fewer matching conditions to impose. By Proposition 4.3, the outer radial solution  $u_O^r$  has Neumann boundary conditions on the elliptic region, and its behavior at  $1 - \epsilon$  can be determined using the Frobenius method.

*Proof of Proposition 4.4.* Because  $u \in C^2(\overline{B_1(0)})$ , the eigenvalue  $\lambda$  must simultaneously verify

$$\begin{aligned} \lim_{r \rightarrow (1-\epsilon)^-} u_I^r(r) &= \lim_{r \rightarrow (1-\epsilon)^+} u_O^r(r) \\ \lim_{r \rightarrow (1-\epsilon)^-} (u_I^r)'(r) &= \lim_{r \rightarrow (1-\epsilon)^+} (u_O^r)'(r). \end{aligned}$$

By (4.6) and Proposition 4.1, these two conditions guarantee that  $u^r$  is  $C^2$  in a neighborhood of  $1 - \epsilon$  and hence  $C^2(\overline{B_1(0)})$ . Because  $\lambda$  is nonnegative and (4.4) is singular near  $r = 0$ , the inner solution is a bounded

Laplacian eigenfunction of frequency  $\sqrt{8\lambda}$ , i.e. a Bessel function of the first kind. For  $u$  to be nontrivial, the following matrix

$$\begin{pmatrix} J_\nu(\sqrt{8\lambda}(1-\epsilon)) & -u_O^r(1-\epsilon) \\ \sqrt{8\lambda}J'_\nu(\sqrt{8\lambda}(1-\epsilon)) & -(u_O^r)'(1-\epsilon) \end{pmatrix}$$

must have zero determinant. This condition equates eigenvalues to roots of the desired transcendental equation.  $\square$

In combination, (4.7) and (4.8) alongside Proposition 4.4 provide a method for determining eigenvalues of  $D_\epsilon$  on the disc. As displayed in Section 5, the analytic predictions match numerical expectations. The eigenvalues also share a variational interpretation under the requirement that each eigenfunction be in  $C^2(\overline{B_1(0)})$ . If we define the energy functional

$$E(f) = \frac{\int_0^{1-r_0} p(1-r)|f'(r)|^2 dr - \nu^2 \int_0^{1-r_0} q(1-r)|f(r)|^2 dr}{\int_0^{1-r_0} w(1-r)|f(r)|^2 dr} \quad (4.10)$$

over all  $f$  such that  $E(f)$  is finite, then the minimizers of  $E$  on orthogonal subspaces of  $L^2([0, 1-r_0], w)$  are solutions of (4.6) with Neumann boundary conditions [3, Ch. 6], in the sense that

$$\lim_{r \rightarrow 1-r_0} p(1-r)f'(r) = 0.$$

Note that the integrals in (4.10) are purely radial because the eigenfunctions of  $D_\epsilon$  are separable and any angular contribution scales out. The eigenfunctions are therefore orthogonal in  $L^2(M_+, w)$  and likewise minimize the functional  $\langle D_\epsilon f, f \rangle_{L^2(M_+, w)}$  as given in (1.10). The Neumann boundary condition matches that established in Section 3 on the unit interval, and hence Theorem 1.4 holds on the disc.

## 5. NUMERICAL COMPARISON

In this section, we provide numerical evidence of eigenvalue convergence when  $D_\epsilon$  is defined on the interval or disc. We also compare eigenvectors of  $I - W$  with eigenfunctions of  $D_\epsilon$  for small  $\epsilon$ . The eigenvectors can be explicitly computed with the regularization in (2.4), and the eigenfunctions can be approximated using the Frobenius methods presented in Propositions 3.2 and 4.3.

On the interval, Proposition 3.4 provides an explicit equation for the analytic eigenvalues in terms of the left solution  $u_L$ . By imposing quasi-Neumann boundary conditions (1.8) on the elliptic region, there exists a unique local solution in the boundary layer that can be approximated to any level of precision via (3.4) and (3.5). In this manner, the analytic eigenvalues featured in this section are gathered using a 12-term Frobenius series representation of  $u_L$  in Proposition 3.4. Any additional terms in the series result in changes beyond the significant figures presented.

In Figure 2, we present the first 5 eigenvectors of  $I - W$  on the unit interval with  $\epsilon = 0.05$ . The first eigenvector is constant, as anticipated in Section 2, and the other eigenvectors resemble Laplacian eigenfunctions. In Figure 3, we determine the eigenvalues of  $I - W$  on the interval under variance in  $n$ , the number of sampled data points, and compare with the analytic eigenvalues predicted by Proposition 3.4. The relative errors, weighted to mirror Corollary 3.5, are also featured in Figure 3.

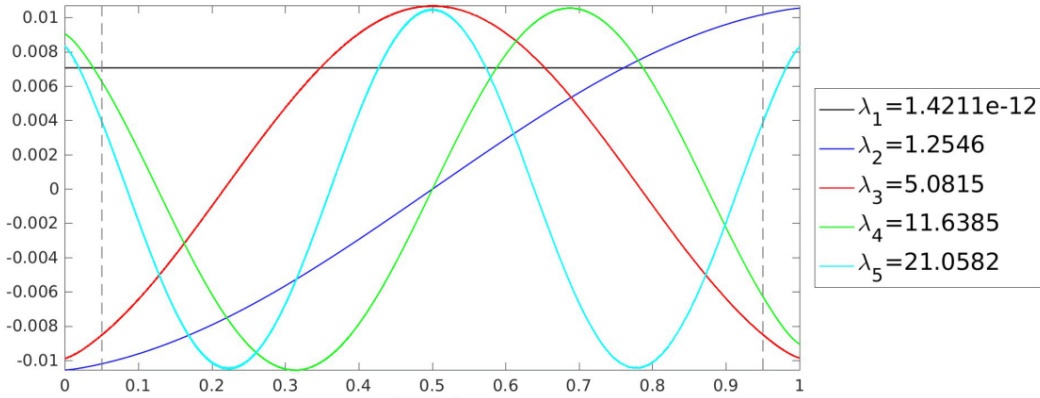


FIGURE 2. For  $\epsilon = 0.05$ , the first 5 eigenvectors of  $I - W$  sampled on 20,000 points in the interval are plotted above. Each is labeled with the respective eigenvalue, appropriately scaled by  $\epsilon^{-2}$  according to (1.2).

**Remark 5.1.** In [15, Fig.5], Wu and Wu display the first 5 eigenvectors of  $I - W$  sampled on 8,000 points in the interval with  $\epsilon = 0.01$ . They discuss several irregularities that we believe arise due to the small number of data points relative to  $\epsilon$ . In particular, the eigenvector irregularity in the boundary layer is not present in Figure 2.

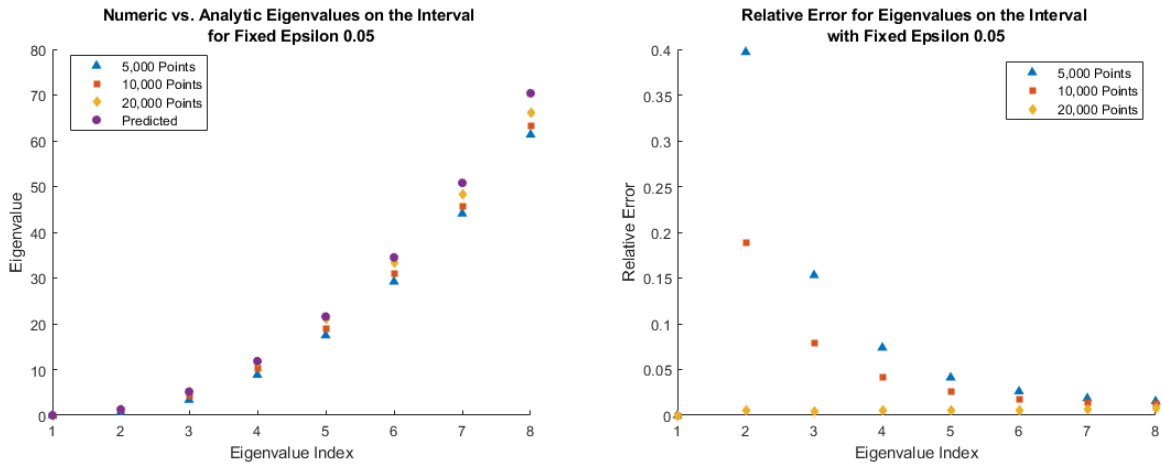


FIGURE 3. In the left figure, the first 8 eigenvalues of  $I - W$  are plotted for different data set sizes and fixed  $\epsilon = 0.05$ . We consider eigenvalue sequences corresponding to 5,000 points, 10,000 points, and 20,000 points before plotting the analytic expectation to display convergence. In the right figure, we plot the relative errors  $|\lambda_j(I - W) - \lambda_j(D_\epsilon)| |\lambda_j(D_\epsilon)|^{-3/2}$  for each eigenvalue sequence.

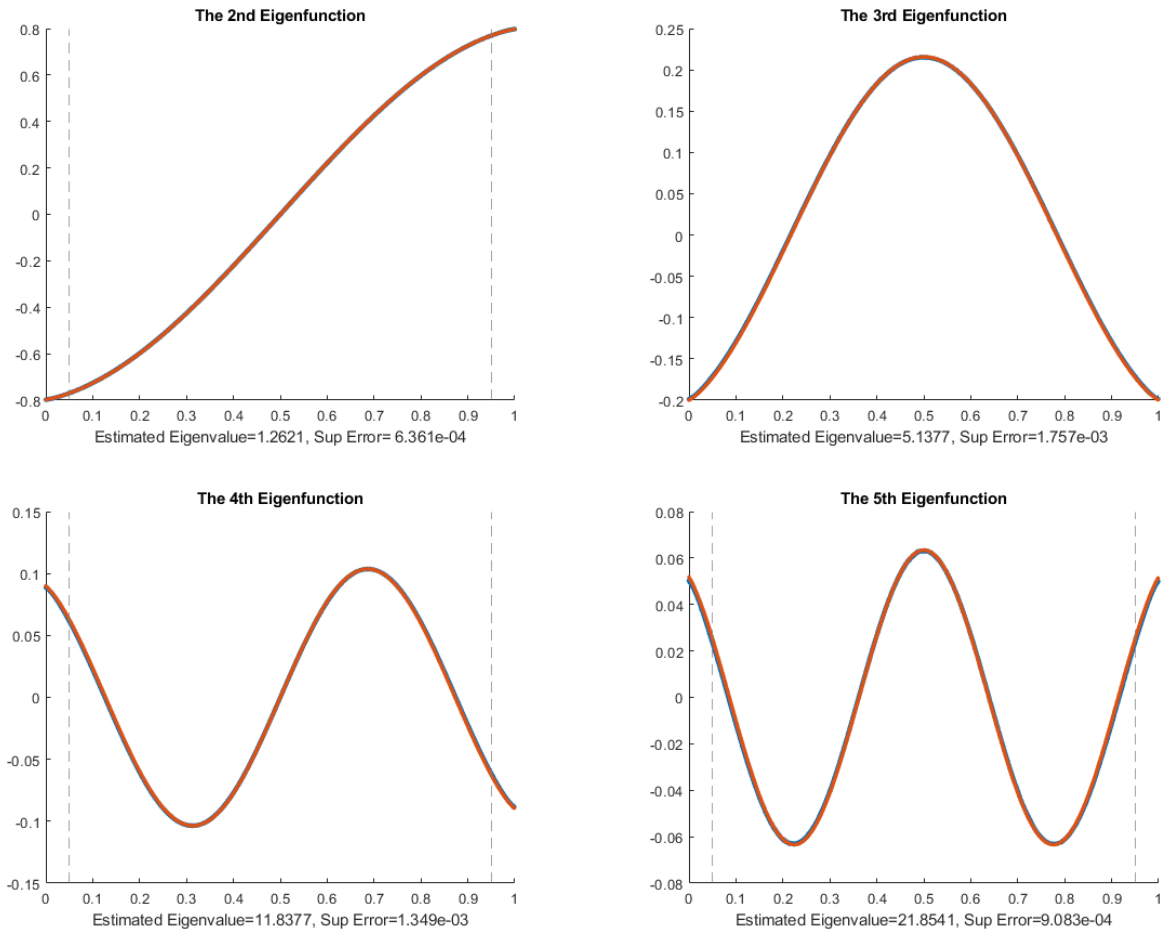


FIGURE 4. For  $\epsilon = 0.05$ , several eigenfunctions of  $D_\epsilon$  with quasi-Neumann boundary conditions (1.8) plotted above. Each eigenfunction has been discretized over 20,000 points and is normalized to minimize error with the corresponding eigenvector of  $I - W$ , featured in Figure 2. From top left to bottom right, we display the 2nd, 3rd, 4th, and 5th eigenfunctions, each labeled with the sup error (when compared with the corresponding eigenvector of  $I - W$ ) and analytically-predicted eigenvalue

On the disc, Proposition 4.4 similarly provides an equation for the analytic eigenvalues in terms of the outer solution  $u_{\mathcal{O}}^r$  with quasi-Neumann boundary conditions (1.9) on the elliptic region. We use (4.7) and (4.8) to construct a 12-term Frobenius series for the local solution in the boundary layer and gather eigenvalues using Proposition 4.4. For comparison, eigenvalues and eigenvectors of  $I - W$  are featured in Figure 5. Note that each eigenvector appears separable on the disc, with integer angular frequency. The first eigenvector is constant, as anticipated in Section 2, and the other eigenvectors resemble Laplacian eigenfunctions on the disc.

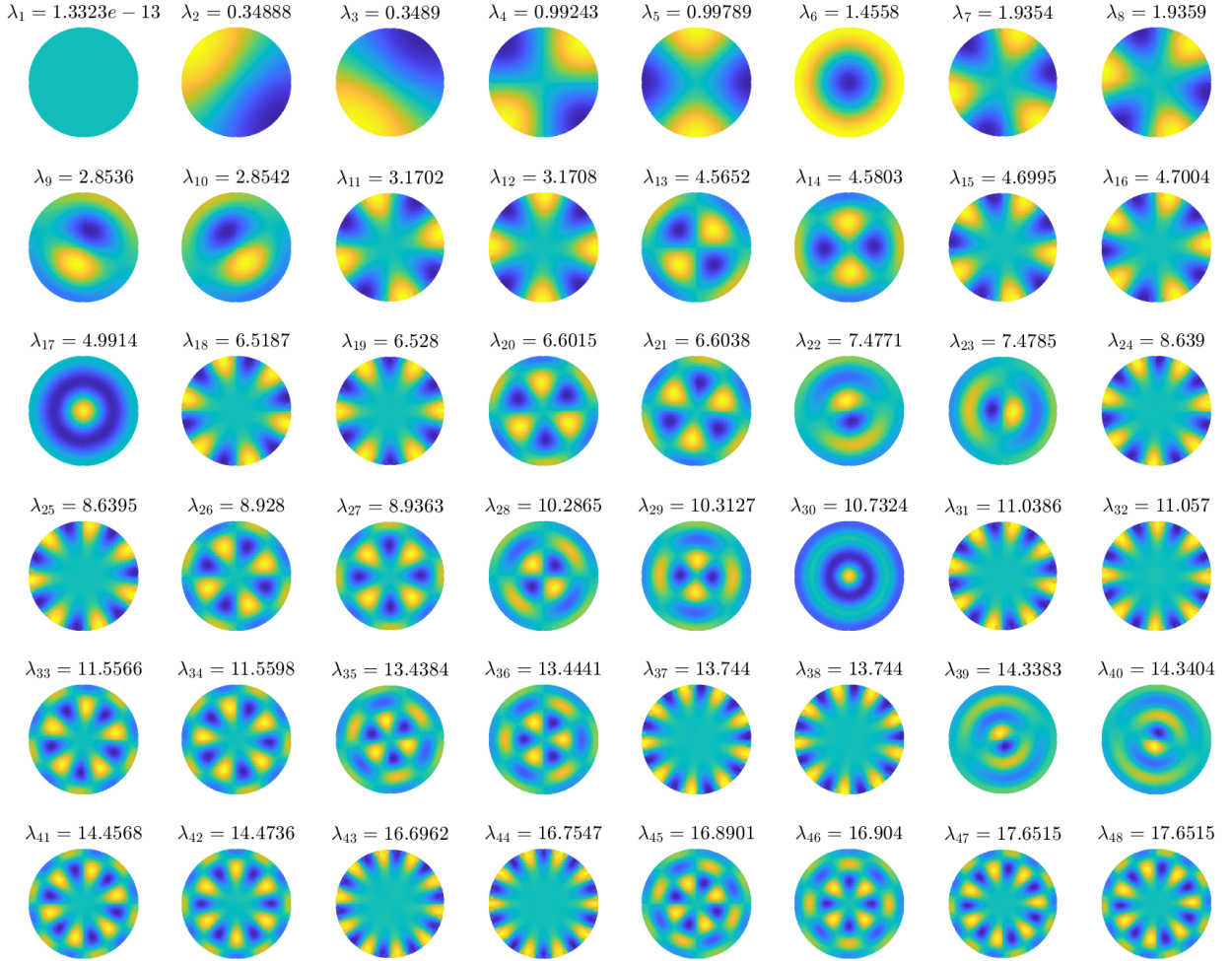


FIGURE 5. For  $\epsilon = 0.05$ , the first 48 eigenvectors of  $I - W$  sampled on 160,000 points in the disc are plotted from top left to bottom right. Each is labeled with the respective eigenvalue, appropriately scaled by  $\epsilon^{-2}$  according to (1.2).

In Figure 6, we let  $\epsilon = 0.05$  and test an increasing sequence in  $n$ , the number of data points from which the LLE matrix  $W$  is constructed. In particular, we let  $\{x_j\}_{j=1}^n$  form a grid in  $[-1, 1] \times [-1, 1]$  and remove points for which the norm is greater than 1. Note that by taking  $n$  too large, we leave the supercritical regime (1.1), and the eigenvectors lose any resemblance to separable functions on the disc. To accompany the evidence of eigenvalue convergence, we also display several eigenfunctions of  $D_\epsilon$  in Figure 7.

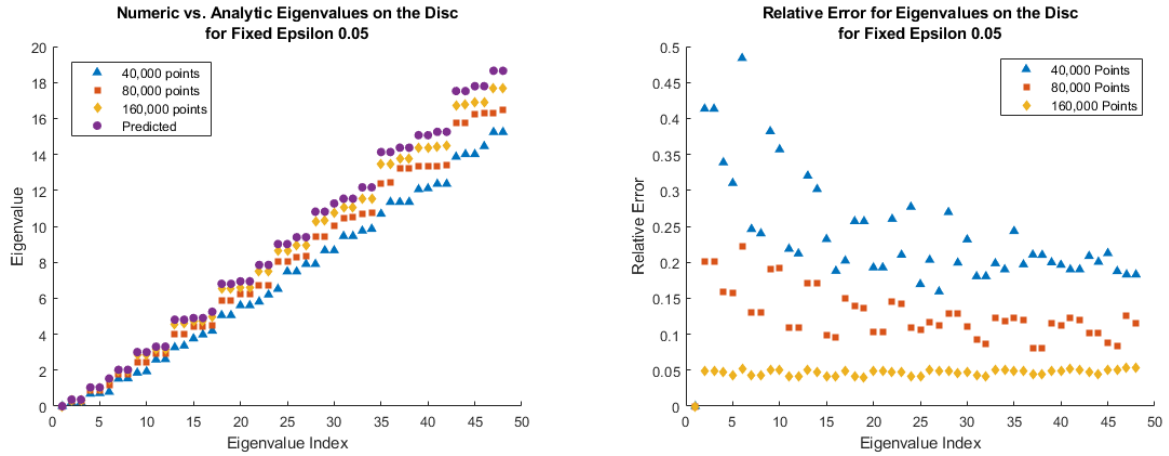


FIGURE 6. In the left figure, the first 48 eigenvalues of  $I - W$  are plotted for different data set sizes and fixed  $\epsilon = 0.05$ . We consider eigenvalue sequences corresponding to 40,000 points, 80,000 points, and 160,000 points before plotting the analytic expectation to display convergence. In the right figure, we plot the standard relative errors  $|\lambda_j(I - W) - \lambda_j(D_\epsilon)| |\lambda_j(D_\epsilon)|^{-1}$  for each eigenvalue sequence.

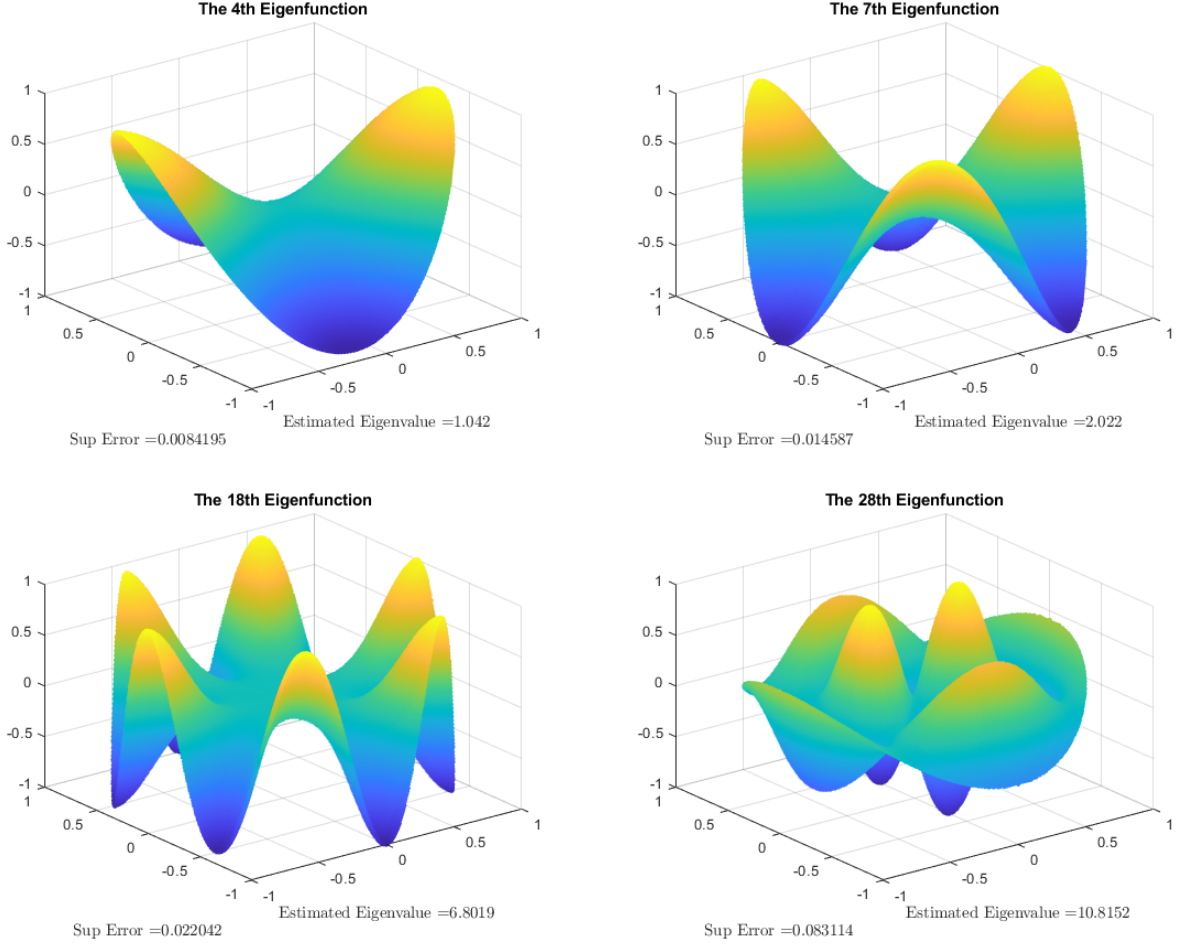


FIGURE 7. For  $\epsilon = 0.05$ , several eigenfunctions of  $D_\epsilon$  with quasi-Neumann boundary conditions (1.9) are plotted above. Each eigenfunction has been discretized over 160,000 points and is rotated and normalized to minimize error with the corresponding eigenvector of  $I - W$ , featured in Figure 5. From top left to bottom right, we display the 4th, 7th, 18th, and 28th eigenfunctions, each labeled with the sup error (when compared with the corresponding eigenvector of  $I - W$ ) and analytically-predicted eigenvalue.

## 6. PROOF OF THEOREM 1.6.

In this section, we use a technique from calculus of variations [12, Ch. 7] to recover quasi-Neumann boundary conditions from a min-max principle governed by Definition 1.5 and prove Theorem 1.6. Let  $M$  be a smooth, compact Riemannian manifold with smooth boundary and let  $D_\epsilon$  be admissible on  $M$ . Unless otherwise stated, we work in the Hilbert space  $L^2(M_+, w)$  where  $M_+$  is the elliptic region in (1.5) and  $w$  is given in Definition 1.5. Set

$$V = \{v \in L^2(M_+, w) : \langle D_\epsilon v, v \rangle < \infty\}$$

and suppose that the  $j$ th eigenvalue of  $D_\epsilon$  on  $M$  can be written

$$\lambda_j = \max_{v_1, \dots, v_{j-1} \in L^2(M_+, w)} \left\{ \min_{v \in V \cap \{v_1, \dots, v_{j-1}\}^\perp \setminus \{0\}} \frac{\langle D_\epsilon v, v \rangle}{\langle v, v \rangle} \right\}.$$

Given 1.10, the minimum over each orthogonal subspace is attained by solutions to (1.3) on  $M_+$ . Let  $u$  be an eigenfunction of  $D_\epsilon$  with  $\|u\| = 1$  and set

$$J_v(t) = \frac{\langle D_\epsilon(u + tv), u + tv \rangle}{\|u + tv\|}$$

for  $v \in V \cap \{v_1, \dots, v_{j-1}\}^\perp \setminus \{0\}$ . Then, because  $u$  is a minimizing function and  $A_\epsilon$  is symmetric,

$$\frac{1}{2} \frac{d}{dt} J_v(t) \Big|_{t=0} = \operatorname{Re} \langle D_\epsilon u, v \rangle - J_v(0) \operatorname{Re} \langle u, v \rangle = 0. \quad (6.1)$$

In particular, (6.1) holds true for arbitrary  $v \in V \cap \{v_1, \dots, v_{j-1}\}^\perp \setminus \{0\}$ . By separating (6.1) into interior and boundary integrals, we recover an Euler Lagrange equation dictating (1.3) on  $M_+$  with  $\lambda = J_v(0)$ . To determine the boundary conditions that the eigenfunctions satisfy, consider the first term in (1.10),

$$\begin{aligned} \frac{1}{2(d+2)} \int_{M \setminus M_\epsilon} \nabla u(x) \overline{\nabla v(x)} dv_g &= - \frac{1}{2(d+2)} \int_{M \setminus M_\epsilon} \Delta u(x) \overline{v(x)} dv_g \\ &+ \frac{1}{2(d+2)} \int_{\partial M_\epsilon} \frac{\partial u}{\partial \nu}(x) \overline{v(x)} d\sigma \end{aligned} \quad (6.2)$$

where  $d\sigma$  is the measure on  $\partial M_\epsilon$  and  $\nu$  is the outward-pointing unit normal along the boundary. According to [15],  $D_\epsilon$  is equal to the Laplacian scaled by  $\frac{1}{2(d+2)}$  outside the boundary layer, and so the interior integral in (6.2) agrees with  $\langle D_\epsilon u, v \rangle_{L^2(M \setminus M_\epsilon)}$ . Meanwhile, by applying integration by parts to the second term in (1.10), we find

$$\begin{aligned} \int_{M_+ \cap M_\epsilon} p(x_d) \frac{\partial u}{\partial x_d}(x) \overline{\frac{\partial v}{\partial x_d}(x)} dx &= - \int_{M_+ \cap M_\epsilon} \frac{\partial}{\partial x_d} \left( p(x_d) \frac{\partial u}{\partial x_d}(x) \right) \overline{v(x)} dx \\ &+ p(\epsilon) \int_{\partial M_\epsilon} \frac{\partial u}{\partial x_d}(x', \epsilon) \overline{v(x', \epsilon)} dx' \\ &- p(x_+) \int_{\partial M_+} \frac{\partial u}{\partial x_d}(x', x_+) \overline{v(x', x_+)} dx' \end{aligned} \quad (6.3)$$

where  $(x', x_d)$  denotes the Fermi coordinates in  $M_\epsilon$  and  $x_+$  denotes the  $d$ th Fermi coordinate for points along  $\partial M_+$ . The interior integral in (6.3) captures the degenerate behavior of  $D_\epsilon$  in  $M_\epsilon$ . Because  $D_\epsilon$  is admissible, the boundary integrals in (6.2) and (6.3) sum to

$$-p(x_+) \int_{\partial M_+} \frac{\partial u}{\partial x_d}(x', x_+) \overline{v(x', x_+)} dx'. \quad (6.4)$$

By construction,  $-\frac{\partial}{\partial x_d}$  is the (outward) normal derivative on  $M_+$ , and by (6.1), we can set (6.4) equal to zero. Because  $v$  is arbitrary, we conclude that

$$p(x) \frac{\partial u}{\partial x_d}(x) = 0$$

for  $x$  along  $\partial M_+$ . Thus,  $u$  has quasi-Neumann boundary conditions on the elliptic region (1.5), and Theorem 1.6 holds.

## APPENDIX A. A VARIATIONAL CONVERGENCE EXAMPLE

In this section, we demonstrate how the higher order correction in (1.2) might force a regularity condition on the eigenfunctions of the leading order operator  $D_\epsilon$  on the unit interval. As shown in Lemma 3.2, absent boundary conditions, there are two linearly independent solutions to (1.3) in the boundary layer. Both solutions are smooth almost everywhere, meaning there is zero probability of sampling either function at a point of low regularity. However, by taking  $\epsilon$  to be supercritical with respect to the sample size (1.1), it is guaranteed that a subset of the boundary layer will be sampled in the LLE algorithm. We provide a



condition for which eigenvalue convergence may be penalized by the presence of singular points near this subset.

According to (1.2), the matrix  $I - W$  behaves like the differential operator  $D_\epsilon$  with a correction. To the author's knowledge, a precise description of this correction is unknown, although the derivation in [15, Appendix F.] indicates that it is a linear differential operator of degree no less than three. Without any imposed regularity, consider the differential operator  $\widetilde{D}_\epsilon$  given by

$$\widetilde{D}_\epsilon f(x) := \phi_2(x)f''(x) + \phi_1(x)f'(x) + \epsilon \sum_{j=3}^J \phi_j(x)f^{(j)}(x) \quad (\text{A.1})$$

where  $\phi_1, \phi_2$  are the piecewise functions in (3.1) and  $J \in \mathbb{N}$ . Suppose each  $\phi_j$  is uniformly bounded on  $[0, 1]$  and satisfies the symmetry condition

$$\phi_j(x) = (-1)^j \phi_j(1-x).$$

This operator is constructed to be a perturbation of  $D_\epsilon$  in (3.1) and remain consistent with properties of the LLE matrix discussed in Section 2. If  $u$  is an eigenfunction of  $\widetilde{D}_\epsilon$  in the weak sense, normalized in  $L^2(M_+, w)$ , then the corresponding eigenvalue  $\tilde{\lambda}$  can be written

$$-\int_{x_0}^{1-x_0} (p(x)u'(x))' \overline{u(x)} dx + \epsilon \sum_{j=3}^J \int_{x_0}^{1-x_0} w(x)\phi_j(x)u^{(j)}(x)\overline{u(x)} dx \quad (\text{A.2})$$

where  $p, w$  are given in Proposition 3.1. Note that, so long as each integral in (A.2) is finite,  $\tilde{\lambda}$  begins to resemble (3.6) as  $\epsilon \rightarrow 0$ . However, there are conditions on the coefficients  $\phi_j$  in (A.1) for which only one function in Proposition 3.2 allows (A.2) to remain finite.

**Assumption A.1.** *There exists some  $j \in \{3, \dots, J\}$  and some  $0 \leq k \leq j - 2 + (4 + 2\sqrt{3})\epsilon$  such that*

$$\lim_{x \rightarrow x_0^+} \phi_j(x)(x - x_0)^{-k}$$

*is finite and nonzero.*

Under this assumption, integrability issues arise in (A.2) whenever  $u$  behaves asymptotically like  $u_{\text{Dir}}$  from Proposition 3.2 near  $x_0$ . This is made precise by the following statement.

**Lemma A.2.** *Let  $f$  be defined as*

$$f(x) = \sin \beta u_{\text{Dir}}(x) + \cos \beta u_{\text{Neu}}(x)$$

*for some  $\beta \in [0, 2\pi)$ . Then*

$$\langle \widetilde{D}_\epsilon f, f \rangle_{L^2(M_+, w_1)} < \infty$$

*if and only if  $\beta = 0$ .*

Under Assumption A.1, the eigenvalues of  $\widetilde{D}_\epsilon$  converge variationally to the eigenvalues of  $D_\epsilon$  if and only if Neumann boundary conditions are imposed on the elliptic region in the limit. Equivalently, this requires eigenfunctions in  $C^2([0, 1])$ .

*Proof of Lemma A.2.* Let  $f$  be a linear combination of the Dirichlet and Neumann solutions parametrized by  $\beta \in [0, 2\pi)$ . By Propositions 3.2 and 3.1,

$$\int_{x_0}^{1-x_0} (p(x)f'(x))' \overline{f(x)} dx < \infty$$

for all  $\beta$ . However, while

$$\sum_{j=3}^J \int_{x_0}^{1-x_0} w(x) \phi_j(x) u_{\text{Neu}}^{(j)}(x) \overline{u_{\text{Neu}}(x)} dx < \infty,$$

the same integral blows up if it features any contribution from the Dirichlet solution  $u_{\text{Dir}}$ , for which  $u_{\text{Dir}}^{(j)}(x)$  is asymptotic to  $(x - x_0)^{1-(4+2\sqrt{3})\epsilon-j}$  as  $x \rightarrow x_0^+$ .  $\square$

On the interval, we suspect that the higher order terms in (1.2) takes the form given in (A.1) and that Assumption A.1 holds. For other manifolds, we state the following conjecture regarding the higher order operator.

**Conjecture 2.** *The  $C^2$  regularity condition, as implemented in Theorems 1.1 and 1.2, arises from the weak form of the full operator in (1.2).*

#### REFERENCES

- [1] Ronald Coifman and Stéphane Lafon. Diffusion maps. *Appl. Comput. Harmon. Anal.*, 21(1):5–30, 2006.
- [2] Eric Cosatto and Hans Graf. Sample-based synthesis of photo-realistic talking heads. *Proc. of Comp. Animation*, pages 103 – 110, 1998.
- [3] Richard Courant and David Hilbert. *Methods of Mathematical Physics*, volume Vol. 1. Academic Press, New York-London, 1964.
- [4] Charles Epstein and Rafe Mazzeo. *Degenerate diffusion operators arising in population biology*, volume 185 of *Annals of Mathematics Studies*. Princeton University Press, Princeton, NJ, 2013.
- [5] Alfred Gray. *Tubes*, volume 221 of *Progress in Mathematics*. Birkhäuser Verlag, Basel, second edition, 2004.
- [6] Lance Littlejohn and Anton Zettl. The Legendre equation and its self-adjoint operators. *Electron. J. Diff. Equations*, pages No. 69, 33, 2011.
- [7] Xin Liu, Duygu Tosun, Michael Weiner, and Norbert Schuff. Local linear embedding (lle) for mri based alzheimer’s disease classification. *Neuroimage*, 26(83):148–157, 2013.
- [8] John Malik, Chao Shen, Hau-Tieng Wu, and Nan Wu. Connecting dots: from local covariance to empirical intrinsic geometry and locally linear embedding. *Pure Appl. Anal.*, 1(4):515–542, 2019.
- [9] Mark Naimark. *Linear differential operators. Part II: Linear differential operators in Hilbert space*. Frederick Ungar Publishing Co., New York, 1968.
- [10] Sam Roweis and Lawrence Saul. Nonlinear dimensionality reduction by locally linear embedding. *Science*, 290(5500):2323–2326, 2000.
- [11] Hualei Shen, Tao Dacheng, and Ma Dianfu. Multiview locally linear embedding for effective medical image retrieval. *PLoS One*, 8(12), 2013.
- [12] Bruce van Brunt. *The calculus of variations*. Universitext. Springer-Verlag, New York, 2004.
- [13] Ryan Vaughn, Tyrus Berry, and Harbir Antil. Diffusion maps for embedded manifolds with boundary with applications to PDEs. *Appl. Comput. Harmon. Anal.*, 68:Paper No. 101593, 38, 2024.
- [14] Hau-Tieng Wu and Nan Wu. Think globally, fit locally under the manifold setup: asymptotic analysis of locally linear embedding. *Ann. Statist.*, 46(6B):3805–3837, 2018.
- [15] Hau-Tieng Wu and Nan Wu. When locally linear embedding hits boundary. *J. Mach. Learn. Res.*, 24:Paper No. [69], 80, 2023.
- [16] Chao Yao, Ya-Feng Liu, Bo Jiang, Jungong Han, and Junwei Han. LLE score: a new filter-based unsupervised feature selection method based on nonlinear manifold embedding and its application to image recognition. *IEEE Trans. Image Process.*, 26(11):5257–5269, 2017.
- [17] Maozhu Zhang, Jiong Sun, and Anton Zettl. Eigenvalues of limit-point Sturm-Liouville problems. *J. Math. Anal. Appl.*, 419(1):627–642, 2014.

*Email address:* ahlyons@email.unc.edu

DEPT. OF MATHEMATICS, UNC-CH, 418 PHILLIPS HALL, CHAPEL HILL, NC 27599-3250, USA